Proceedings of *AmeriMech* Symposium

Dynamics of Periodic Materials and Structures

Sponsored by

3 – 4 April 2014

Georgia Tech Hotel and Conference Center

Atlanta, Georgia, USA

Contents

Preface

Welcome to Atlanta!

The objective of this inaugural AmeriMech symposium is to bring together junior and senior researchers working on periodic materials and structures in order to a) share recent and emerging developments in periodic structures and materials (cellular/lattice materials; acoustic metamaterials; phononic crystals), and b) identify areas requiring new developments in theory, manufacturing technologies, and applications.

The organizers would like to acknowledge generous financial support from the United States National Committee on Theoretical and Applied Mechanics (USNCTAM), the National Science Foundation (NSF), the University of British Columbia and Georgia Tech. We would also like to thank USNCTAM representatives Prof. G. Ravichandran (California Institute of Techology) for accepting our proposal to organize this symposium and Prof. Wayne Chen (Purdue University) for overseeing its execution.

We hope you will find in this symposium an opportunity to foster new connections and forge new directions in your research on dynamics of periodic materials and structures. We look forward to two days of stimulating research presentations. Please check the symposium website http://blogs.ubc.ca/amerimech2014/program/ shortly after the symposium's conclusion for electronic copies of the proceedings and the presentations. Last and not least, thank you for attending and making this event a success!

– M.J. Leamy & A.S. Phani
April, 2014

Dynamic Response of Periodic Materials and Structures

April 3-4, 2014, Atlanta, Georgia, USA

Symposium Agenda for 3 April 2014 in Conference Room A

Time	Speaker	Title
7.30 – 8.45		Breakfast & Registration
8.45 – 9.00	Organizers	Welcome and introductory remarks
		Wave Propagation
9.00 – 9.30	A.N. Norris	Dynamics of pentamode structures using beam theory
9.30 – 10.00	M. Ruzzene	Wave propagation in geometrically reconfigurable magneto-elastic meta-structures
10.00 – 10.30	A.S. Phani	Tailoring bandgaps and vibroacoustic response of periodic materials
		10.30 – 11.00
		Coffee
11.00 – 11.30	N. X. Fang	Quest for flexible acoustic circuitry with acousto-elastic metamaterials
11.30 – 12.00	S. Gonella	Packet modulation and mode hopping in nonlinear periodic structures
12.00 – 12.30	N. Boechler	Microscale granular acoustic metamaterials
		12.30 – 1.30
		Lunch
		Phonon & Thermal Transport
1.30 – 2.00	A.J. McGaughey	Phonon transport in periodic materials with feature sizes of 1 nm to 1μm
2.00 – 2.30	I. El-Kady	Thermal transport in micro-scale phononic crystals: observation of coherent phonon scattering at room temperature and its implications to thermoelectrics
2.30 – 3.00	M.I. Hussein	Nanophononic metamaterial: slowing down heat transfer by mechanical vibrations
		3.00 – 3.30
		Coffee
3.30 – 4.00	P. Deymier	Phononic crystals supporting Fermion-like rotational modes
4.00 – 4.30	M.J. Leamy	Amplitude-dependent wave devices based on nonlinear periodic materials
4.30 – 5.00	M. Maldovan	Phonon heat management by periodic materials: how to treat heat like sound
		5.00 – 6.30
		Poster Session
		7.00 pm
		Dinner in Conference Room 2

Symposium Agenda for 4 April 2014 in Conference Room A

Time	Speaker	Title
7.00 – 8.30		Breakfast
		Multifunctional Applications
8.30 – 9.00	T. Schaedler	Hollow microlattices: energy absorption and damping performance
9.00 – 9.30	L. Valdevit	Optimal design of stiff and lossy multiphase cellular materials
9.30 – 10.00	C. Steeves	Hybrid polymer-nanometal lattices
10.00 – 10.30	D. Pasini	Multiobjective optimization of a graded lattice for hip replacement: integration of manufacturing and bone growth requirements
		10.30 – 11.00
		Coffee
11.00 – 11.30	K. Bertoldi	Harnessing geometric and material nonlinearities to design tunable phononic crystals and acoustic metamaterials
11.30 – 12.00	A. Baz	Active acoustic and structural metamaterials
12.00 – 12.30	G. Huang	Coupled vibroacoustic modelling of membrane-type metamaterials

12.30 – 1.30
Lunch
1.30 – 2.30
Panel discussion and concluding remarks

Sponsors

Dynamics of pentamode structures using beam theory

Andrew N. Norris[1], Adam J. Nagy[1], Xiaoshi Su[1], Anton A. Kutsenko[2]

[1] *Rutgers University, Mechanical and Aerospace Engineering, Piscataway NJ 08854-8058, USA*
[2] *Institut de Mécanique et d'Ingénierie, Université de Bordeaux, UMR CNRS 5469, Talence 33405, France*
norris@rutgers.edu, adnagy@eden.rutgers.edu,, xiaoshi.su@rutgers.edu, aak@nxt.ru

Abstract: Dynamic modeling of elastic structures with pentamode-like properties is considered via Bloch-Floquet analysis using a beam model for the periodic lattice. The simple beam theory includes longitudinal and flexural waves, and leads to a semi-analytical solution which is compared against FEM simulations for wave dispersion in two and three dimensional structures. Numerical comparisons indicate that the beam model provides very good accuracy for the lower modes, and show the macroscopic shear modulus to be relatively small as compared to the bulk modulus, characteristic of quasi-pentamode behavior.

Pentamode materials (PMs) were proposed[1,2] as limiting cases of elastic solids with five easy modes, analogous to inviscid compressible fluids but without the ability to flow. Recent interest has resulted from the observation[3,4] that PMs provide the potential for realizing transformation acoustics[5]. A two-dimensional aluminum honeycomb PM structure, called Metal Water[6], approximates the acoustical properties of water by providing the correct density and bulk modulus in the quasistatic limit, with small shear. At higher frequency Metal Water also displays Floquet branches with negative group velocity that provide the possibility for negative index of refraction[7]. Recent work includes the analysis of anisotropic PMs in 2D[8] and 3D[9], and fabrication of 3D PMs[10,11,12].

PMs, whether 2D[6] or 3D[10], are lattice structures comprising long, thin members in order to reduce the shear while maintaining "compressibiility". It is natural then to expect that thin beam theory simultaneously provides an accurate and simple model for the quasi-static and dynamic properties of the PM. The purpose of this paper is to verify this expectation though explicit examples.

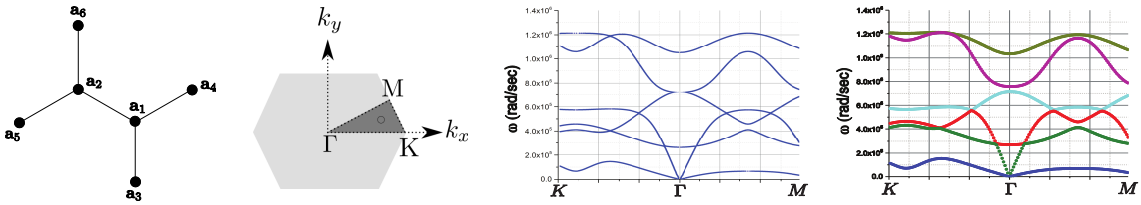

(a) (b) (c) (d)

Figure 1: Dispersion curves of the regular hexagonal lattice of aluminum struts, *E=69 GPa*, *v=1/3*, *ρ=2700 kg/m*^{3},rod length *l=4.39 mm*, thickness *0.35 mm*. (a) Unit cell. (b) Irreducible Brillouin zone. (c) The first 6 branches using beam theory. (d) Curves calculated using FEM.

Considering lattice structures with unit cell such as Figure 1 (a) we take a force balance at node $\boldsymbol{a}_i$

$$\sum_{j\in N_i} \boldsymbol{f}_{ij} = -\omega^2 \boldsymbol{M}_i \boldsymbol{u}_i, \qquad \boldsymbol{M}_i = \mathrm{diag}(m_i, m_i, I_i), \tag{1}$$

$\boldsymbol{f}_{ij}$ is the force at $\boldsymbol{a}_i$ from the rod connecting points $\boldsymbol{a}_i$ and $\boldsymbol{a}_j$, m_i and I_i are mass and moment of inertia of joint $\boldsymbol{a}_i$, N_i is the set of points connected to $\boldsymbol{a}_i$ and ω is radial frequency. $\boldsymbol{f}_{ij}$ are found by considering the longitudinal and flexural motion of Euler-Bernoulli beams. Bloch-Floquet periodicity conditions are enforced on the unit cell, e.g. $\boldsymbol{u}_4 = \boldsymbol{u}_5 e^{i\boldsymbol{k}\cdot(\boldsymbol{a}_4-\boldsymbol{a}_5)}$, for wavevector $\boldsymbol{k}$, resulting in the eigenvalue problem $\det(\boldsymbol{H}(\omega,\boldsymbol{k}) - \omega^2\boldsymbol{M}) = 0$, where $\boldsymbol{H}(\omega,\boldsymbol{k})$ is a small Hermitian matrix. Figure 1 shows a comparison of the predictions of eq. (2) vs. FEM (COMSOL) for a 2D honeycomb structure. The analysis is easily extended into three dimensional cubic or more complicated lattices such as te-

tragonal. Figures 2 and 3 show comparisons for cubic (strictly not a PM) and tetragonal lattices. In all examples we see the slope of the shear branch is small as compared to the longitudinal.

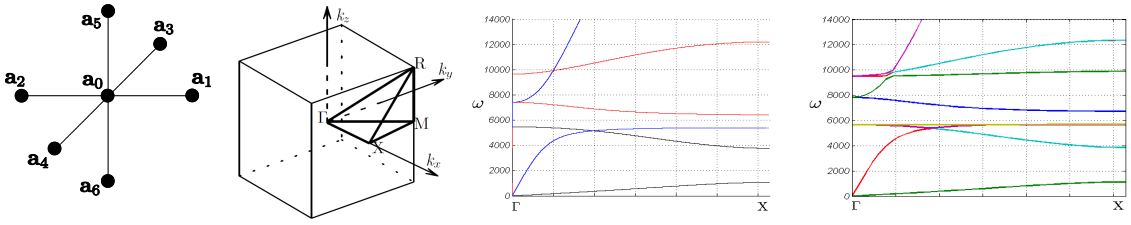

(a) (b) (c) (d)

Figure 2: Dispersion curves of the cubic lattice: *E=70 GPa*, *v=1/3*, *ρ=2700 kg/m*^{3}, *l=250 mm,*rod radius *r=6 mm*. (a) Unit cell. (b) Irreducible Brillouin zone. (c) The first six branches from eq. (2) for ***k*** along the perimeter of the Brillouin zone. (d) Dispersion curves calculated using FEM.

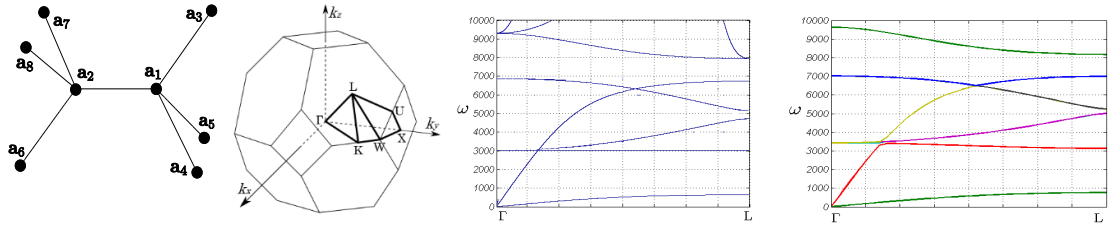

(a) (b) (c) (d)

Figure 3: Dispersion curves of the tetragonal lattice with *E=193 GPa*, *v=1/3*, *ρ=8000 kg/*^{3}, *l=200 mm, r=5 mm*. (a) Unit cell. (b) Irreducible Brillouin zone. (c) The first six branches using eq. (2) for ***k*** along the perimeter of the Brillouin zone. (d) Dispersion curves using FEM.

Acknowledgement: Support from the Office of Naval Research (Multidisciplinary University Research Initiative Grant No. N00014-13-1-0631) is gratefully acknowledged.

References

[1] G.W. Milton and A.V. Cherkaev. Which elasticity tensors are realizable? *J. Eng. Mater. Tech*. **117**(4), 483–493, 1995.
[2] G.W. Milton, *The Theory of Composites*, Cambridge University Press, Cambridge, 2002.
[3] A. N. Norris. Acoustic cloaking theory. *Proc. R. Soc. A*., **464**:2411-2434, 2008.
[4] A.N. Norris. Acoustic metafluids. *J. Acoust. Soc. Am*. **125**(2), 839–849, 2009.
[5] N.H. Gokhale, J.L. Cipolla and A.N. Norris. 2012 Special transformations for pentamode acoustic cloaking. *J. Acoust. Soc. Am*. **132**(4), 2932–2941.
[6] A.N. Norris and A.J. Nagy. Metal Water: A metamaterial for acoustic cloaking. Proceedings of Phononics 2011, Paper Phononics-2011-0037, pp. 112-113, Santa Fe, NM, USA, May 29-June 2, 2011.
[7] A.C. Hladky-Hennion, J.O. Vasseur, G. Haw, C. Croënne, L. Haumesser L and A.N. Norris. Negative refraction of acoustic waves using a foam-like metallic structure. *Appl. Phys. Lett*. **102**(14), 144103, 2013.
[8] C. N. Layman, C. J. Naify, T. P. Martin, D. C. Calvo, and G. J. Orris. Highly-anisotropic elements for acoustic pentamode applications. *Phys. Rev. Lett.,* **111**:024302, 2013.
[9] A. Martin, M. Kadic, R. Schittny, T. Bückmann and M. Wegener. Phonon band structures of three-dimensional pentamode metamaterials. *Phys. Rev. B* **86**, 155116+5, 2012.
[10] M. Kadic, T. Bückmann, N. Stenger, M. Thiel and M. Wegener. On the feasibility of pentamode mechanical metamaterials. *Appl. Phys. Lett.* **100**, 191901, 2012.
[11] R. Schittny, T. Bückmann, M. Kadic and M. Wegener. Elastic measurements on macroscopic three-dimensional pentamode metamaterials. *Appl. Phys. Lett*. **103**(23), 231905+, 2013.
[12] M. Kadic, T. Bückmann, R. Schittny and M. Wegener. Metamaterials beyond electromagnetism. *Rep. Prog. Phy.* **76**(12), 126501+, 2013.

Wave Propagation in Geometrically Reconfigurable Magneto-Elastic Meta-Structures

Marshall Schaeffer[2], Massimo Ruzzene[1,2]

[1] *School of Aerospace Engineering*
[2] *School of Mechanical Engineering,*
ruzzene@gatech.edu

Abstract: The in-plane wave propagation characteristics of two-dimensional (2D) magneto-elastic periodic lattices are investigated. These structures feature the ability to undergo large topological and stiffness changes, which result in dramatic changes in wave propagation characteristics. Such changes are investigated through lumped parameter models which are integrated through nonlinear numerical simulations, and unit cell analysis upon linearization about different equilibrium states.

The mechanical properties of magneto-elastic meta-structures are investigated. These structures are periodic lattices governed by a combination of elastic and magnetic forces. They exhibit tunability by changing magnetization and demonstrate the ability to undergo large topological changes, which allows for further changes in stiffness and equivalent density. Instabilities caused by the highly nonlinear position-dependent characteristics of magnetic interactions are exploited in combination with contact interactions to produce the desired changes in the topology of the structures. The result is multiple stable lattice configurations with very different static and dynamic mechanical properties.

The analysis of magneto-elastic lattices is conducted using a lumped mass system of magnetic particles with both translational and rotational degrees of freedom (Figure 1). Particles within the lattice interact through axial and torsional elastic forces as well as magnetic forces. The behaviour of the periodic lattices about one of their multiple stable equilibrium configurations is investigated through the application of Bloch Theorem, whereby non-nearest neighbour interactions are included to account for the long range effect of the magnetic forces. Fully nonlinear numerical simulations are also conducted to assess the dynamic behavior, the transition from various equilibrium configurations, and the dynamic response changes associated with the topological transitions.

The presented numerical results show how the considered systems are able to conveniently generate double-well potential interactions (Figure 2), which can be exploited to tune or adapt the dynamic behavior of structural assemblies in response to an external stimulus (Figures 3 and 4). Such adaptation may be designed to provide the ability to adaptively guide elastic waves and steer them along desired directions. The considered configurations may be effective at reducing the effects of impacts, or for tunable vibration isolations applications.

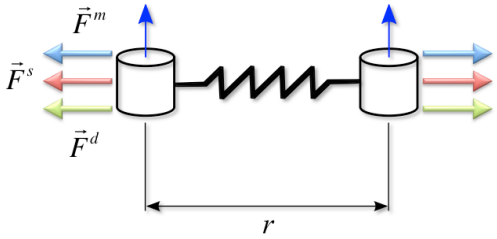

Figure 1: Schematic of interactions between two particles

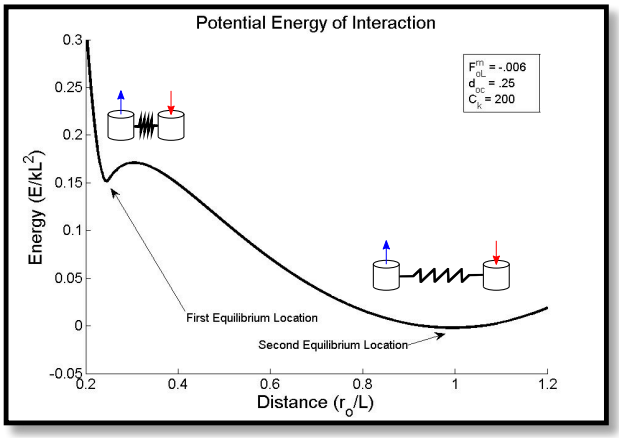

Figure 2: Example of double-well potential of interaction

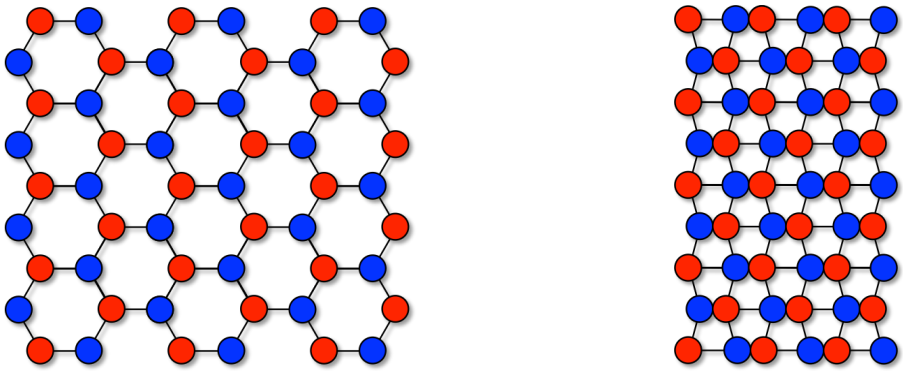

Figure 3: Hexagonal (left) and re-entrant (right) honeycomb lattices corresponding to two equilibrium configurations (Blue and red dots indicate magnets of opposite polarization)

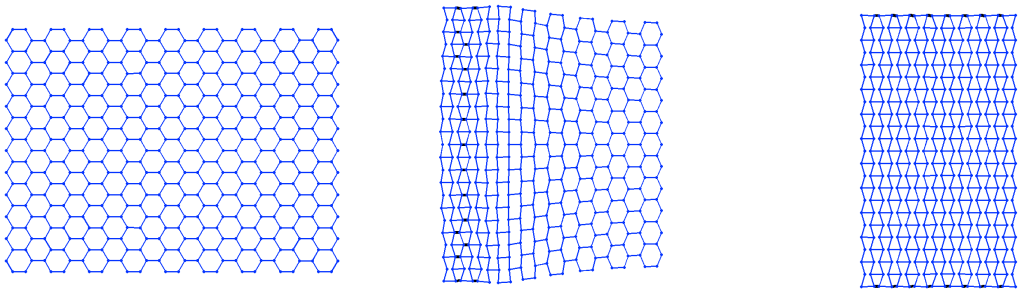

Figure 4: Dynamic transition resulting from the dynamic excitation of an heaxagonal lattices, leading to its reconfiguration as a re-entrant topology.

Tailoring Bandgaps and Vibroacoustic Response of Periodic Materials and Structures

A.Srikantha Phani[1]

[1] *Department of Mechanical Engineering, University of British Columbia, Vancouver, BC, Canada V6T1Z4*
email srikanth@mech.ubc.ca

Abstract: Periodic materials and structures filter waves in frequency and spatial domains. In frequency domain, waves with frequencies falling in an interval (known as bandgap) are forbidden to propagate. Similarly waves have preferential directions of propagation in the spatial domain. Both these filtering characteristics can be exploited in structural applications to control vibration and acoustic response. This talk will focus on the opportunities and challenges in this endeavor using a combination of theory and experiments. Specifically, the importance of unitcell resonances and their prediction using receptance-coupling technique will be demonstrated. The proposed technique does not require the widely used Floquet-Bloch theory.

Modern structural materials are designed to achieve high stiffness, strength, toughness and damping with minimum weight to build efficient structural components used in manufacturing (machine tool structures) and transportation (sandwich panels in naval, aerospace and automotive) industries. The quest to design lightweight materials has first lead to the development of metal and polymeric foams[1,2] and more recently lattice materials[3], and their nano crystalline hybrids[4], and ultralight periodic materials with hollow truss architecture[5]. These new periodic materials are being developed to not only meet the structural efficiency requirements of high specific stiffness and strength, but also achieve other functional characteristics such as thermal insulation of aerostructures, shock resistance, catalysis, and ceramic particle filters in automotive exhaust systems. Deep elastic boundary layers (zero frequency edge/surface waves) have been shown to enhance toughness[6]. In sum, periodic materials and structures increasingly find application as multifunctional structures and more recently as metamaterials and phononic crystals[7].

A characteristic feature of periodic core materials used in sandwich construction, or periodic structures in general, is the phenomenon of bandgaps, where by waves falling in a certain frequency interval are forbidden to propagate. This phenomenon is well known from the pioneering studies of Rayleigh[8] in the context of structural vibrations and Brillouin[9] in the context of solid state physics. Recent studies have shown that the edge frequencies of bandgap are associated with the resonant frequencies of the unit cell under appropriate boundary conditions, see[10, 11] and references therein. This holds true for finite and infinite periodic structures with a symmetric unit cell. Opportunities exist to tailor bandgaps using compressive loads[12], local resonance[13,14] and inertial amplification mechanisms[15]. Thus the location and width of a bandgap can be designed by appropriately changing the unitcell resonance frequencies. Both Bragg and sub-Bragg bandgap widths can thus be tailored. Insights gained from studies on macro-scale periodic structures can be extended to micro and nano-scale periodic materials.

The talk will describe a receptance coupling technique to predict the resonant frequencies of the unitcell and hence the bandgap widths. *This technique does not require the band structure computation using Floquet-Bloch theory as widely used in the current literature to determine bandgaps*. Focusing on waves propagating in a one-dimensional periodic structure, a flexural beam, the bandgap emergence mechanisms will be elucidated. It will be shown that a two-fold periodicity is favorable to enhance simultaneously both the Bragg and the sub-Bragg bandgaps. The talk will conclude with challenges and opportunities in reducing sound transmission loss of sandwich beams by revisiting the trade offs between the structural and the acoustic requirements. Requirements on the core materials for an ideal sandwich structure will be deduced by considering double-wall resonance and coincidence effects arising from fluid-structure wave interactions.

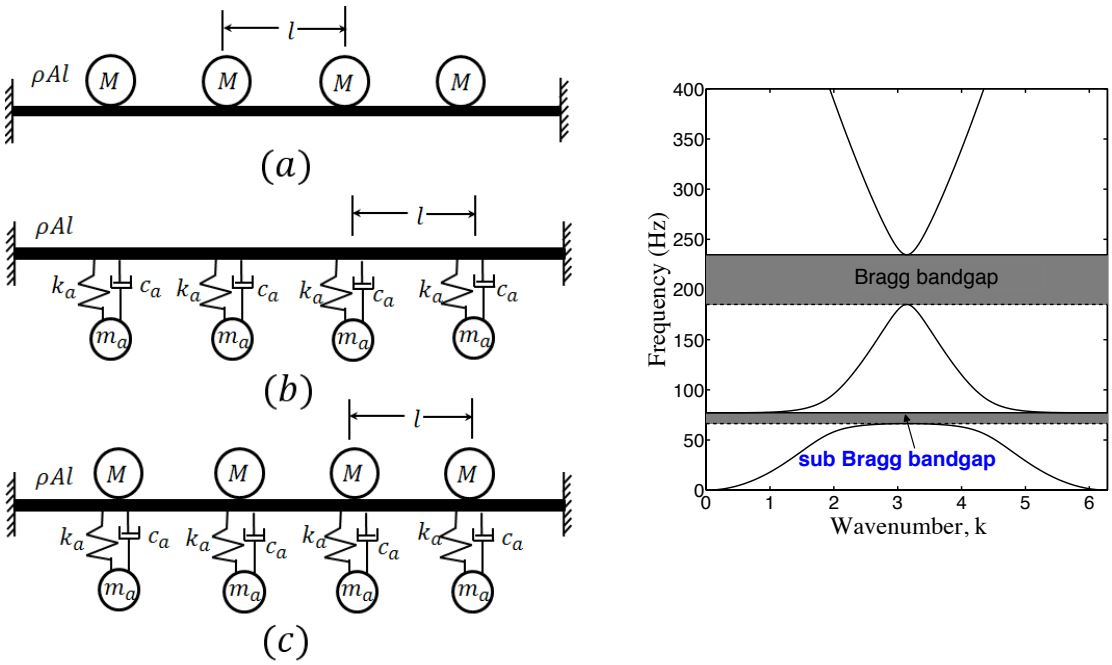

Figure 1 Three cases of a flexural beam periodic structure (left) and the Bragg and the sub-Bragg bandgaps (right) corresponding to case (c). The dotted and the solid horizontal lines on the right are bandgap (grey area) edges predicted by receptance technique *without* using Floquet-Bloch theory.

References

[1]M. F. Ashby. Hybrids to fill holes in material property space. Philosophical Magazine, 85(26 27): 3235–3257, 2005.
[2]J. Banhart. Light-metal foams—history of innovation and technological challenges. Advanced Engineering Materials, 15(3):82–111, 2013.
[3]N. A. Fleck, V. S. Deshpande, and M. F. Ashby. Micro-architectured materials: past, present and future. Proceedings of the Royal Society A: Mathematical, Physical and Engineering Science, 466 (2121):2495–2516, 2010.
[4] B. Bouwhuis, J. McCrea, G. Palumbo, and G. Hibbard. Mechanical properties of hybrid nanocrystalline metal foams. Acta Materialia, 57(14):4046 – 4053, 2009.
[5] T. A. Schaedler, A. J. Jacobsen, A. Torrents, A. E. Sorensen, J. Lian, J. R. Greer, L. Valdevit, and W. B. Carter. Ultralight metallic microlattices. Science, 334(6058):962–965, 2011.
[6]A. S. Phani and N. A. Fleck. Elastic boundary layers in two-dimensional isotropic lattices. Journal of Applied Mechanics, 75(2):021020, 2008.
[7]P. A. Deymier. Acoustic metamaterials and phononic crystals. Springer, New York, 2013.

[8]L. Rayleigh, "On the maintenance of vibrations by forces of double frequency, and on the propagation of waves through a medium endowed with a periodic structure," Philos. Mag. 24, 145–159 (1887).

[9]L. Brillouin. Wave Propagation in Periodic Structures. Mineola, NewYork: Dover publicaions, inc., second edition, 1953.
[10]A. S. Phani, J.Woodhouse, and N. A. Fleck. Wave propagation in two-dimensional periodic lattices. The Journal of the Acoustical Society of America, 119(4):1995–2005, 2006.
[11]L. Raghavan and A. S. Phani. Local resonance bandgaps in periodic media: Theory and experiment. The Journal of the Acoustical Society of America, 134(3):1950–1959, 2013.
[11] A. S. Phani. Waves, Buckles, and Homoclinics. Proceedings of ASME IMECE 2009, 149–158, 2009.
[13]Z. Y. Liu, X. X. Zhang, Y. W. Mao, Y. Y. Zhu, Z. Y. Yang, C. T. Chan, and P. Sheng. Locally resonant sonic crystals. Science, 289(5485):1734–1736, 2000.
[14]L. Liu and M. I. Hussein.Wave motion in periodic flexural beams and characterization of the transition between Bragg scattering and local resonance. J. Appl. Mech. 79, 011003, 2012.
[15]C. Yilmaz, G.M. Hulbert, and N. Kikuchi.Phononic bandgaps induced by inertial amplification in periodic media. Phys.Rev.B, 76, 054309, 2007.

Quest for flexible acoustic circuitry with acousto-elastic metamaterials

Shengqiang Cai, Tian Gan, Narges Kaynia, Anshuman Kumar, Stephan Rudykh, Jun Xu and Nicholas X. Fang[1]

[1] Department of Mechanical Engineering

Massachusetts Institute of Technology

77 Massachusetts Ave, Cambridge, MA 02139, USA

email: nicfang@mit.edu

Abstract: In this invited talk, we will present our progress in bending and folding acoustic waves in a flexible acoustic circuitry. Motivated by our recent success in cloaking and beam shaping using coordinate transformation in acoustics, we will apply it to elastic and deformable systems, with potential applications such as tailoring the wavefront of the initial compressive shock and the returning tensile shocks through selective deflection, mode transformation, focusing, or enhanced energy dissipation in the structures to mitigate subsequent damage or to direct the blast wave to a subsequent target.

.

The remarkable success of electromagnetic metamaterials stimulated exploration of controlling and manipulation of other form of waves in materials. For example, it is theoretically predicted [1] that acoustic wave in fluids could be bent artificially by providing a desired spatial distribution of anisotropic acoustic elements. However, experimental studies of these exciting ideas based on coordinate transformation have been hindered due to the difficulty in creating suitable materials with proper anisotropic mass density or bulk modulus.

To overcome such challenges, we take the analogy between lumped acoustic elements (pipes and chambers) and electronic circuit elements to construct a new class of metamaterials. When the dimensions of the region in which the sound propagates are much smaller than the wavelength, the phase is roughly constant throughout the element, a lumped-parameter model is appropriate. This transmission line approach enabled ultrasound focusing through a metamaterial network and low-loss and broadband cloaks[2] with the use of non-resonant constituent elements.

However, in order to make these metamaterials with desired properties, complex fabrication techniques are usually required, and the properties of a metamaterial are fixed once it is fabricated. Furthermore, for most materials, the influence of deformation on their acoustic or electromagnetic properties is small and non-controllable. Inspired by recent advancement of flexible electronics, we will present our progress in bending and folding acoustic waves in a flexible acoustic circuitry[3]. Motivated by our recent success in cloaking and beam shaping using coordinate transformation in acoustics, we will apply it to elastic and deformable systems that display strong acousto-elasticity, that is, to tune the acoustic properties of a metamaterial through mechanical deformations.

Such elastic and reconfigurable metamaterials also show potential for tailoring the wavefront of the initial compressive shock and the returning tensile shocks. We will discuss our preliminary modeling work on this end through selective deflection, mode transformation, focusing, or enhanced energy dissipation in the structures to mitigate subsequent damage or to direct the blast wave to a subsequent target.

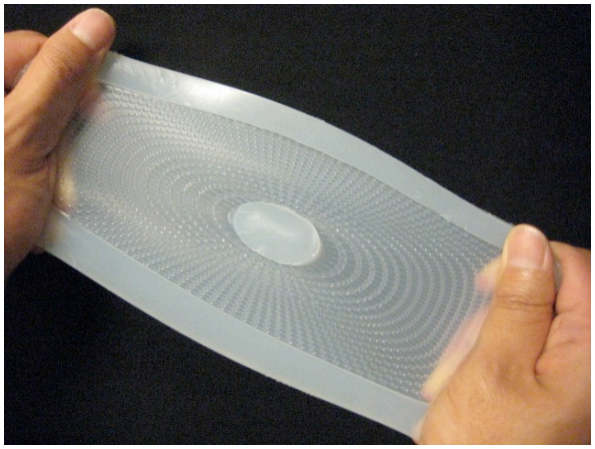

Fig. 1: Deformation of a flexible acoustic circuitry made of acoustic metamaterial network.

References

1. Pendry J .B. and Li Jensen, "An acoustic metafluid: realizing a broadband acoustic cloak", New J. Phys. 101, 15032 (2008)

2. S. Zhang, C. Xia and N. Fang, "Broadband Acoustic Cloak for Ultrasound Waves", Phys. Rev. Lett. 106, 024301 (2011).

3. Cho, S., "INVESTIGATION OF DEFECTS ON ACOUSTIC SCATTERING IN CLOAK BY MOLDING PROCESS", MS Thesis, 2011.

PACKET MODULATION AND MODE HOPPING IN NONLINEAR PERIODIC STRUCTURES

R. Ganesh, S. Gonella[1]

[1] *Department of Civil Engineering, University of Minnesota, Minneapolis, MN, USA*
ramak015@umn.edu, sgonella@umn.edu

Abstract: In this work we explore the wave manipulation capabilities of granular chains and crystals in different regimes of nonlinearity. Our objective is to map the packet distortion and modulation mechanisms and link them to the constitutive, spectral and excitation parameters of the systems. To this end, we identify and monitor metrics of wave propagation that are sensitive to the dispersive and nonlinear parameters. In the strongly nonlinear regime, we exploit the phenomenon of mode hopping to activate multiple functionalities in granular crystals through simple mono-frequency excitations.

Granular chains, like other phononic crystals combining dispersive and nonlinear characteristics, feature substantial wave manipulation capabilities due to their ability to modify the spatial characteristics of traveling waves. In the regime of weak nonlinearity, which corresponds to large values of precompression and/or low amplitudes of excitation, a granular chain essentially behaves like an FPU-α chain (a spring-mass chain with quadratic nonlinearity). In sufficiently dispersive regimes, the spatial manipulation has been found to manifest in the form of a long-wavelength amplitude modulation of the inherent carrier frequency. This effect can be formally described using a multiple scale technique [1] and has been confirmed in a simulation-assisted environment for different dispersive regimes [2]. It has been shown that the variation of the tail amplitude of the long-wavelength modulation, which is chosen as a metric of nonlinearity, features an interesting parameterization with respect to the system and excitation parameters: namely it scales linearly with the coefficient of nonlinearity (function of the precompression and of the exponent of the nonlinear power law), quadratically with the amplitude of the excitation, and cubically with the frequency of excitation. It has been demonstrated that the coefficients of the cubic frequency law can be regarded as invariants of quadratic nonlinearity, as they control the way in which the equivalent quadratic nonlinear features of wave propagation manifest in the behavior of the granular chain.

A richer scenario is observed in the analysis of multiatomic granular systems due to the additional complexity posed by the competition of different inertial parameters. Here we illustrate the problem using the benchmark case of a diatomic granular chain, consisting of two populations of alternating particles. The diatomic chain features two modes of wave propagation (acoustic and optical) separated by a bandgap. The key questions are: what is the effect of the mass contrast on the characteristics of wave propagation? How does this effect interplay with other system parameters, such as frequency and nonlinearity? Are packet modulation mechanisms observed across the entire modal structure of the lattice? We find that a long-wavelength amplitude modulation is observed with similar characteristics to the monoatomic chain case and is observed regardless of the frequency of excitation and the specific mode that is activated. A similar parameterization of the tail amplitude with respect to nonlinearity, amplitude and frequency is obtained; on top of that, a further cubic dependence of the maximum tail amplitude with respect to the mass contrast is recovered. The coefficients of this cubic law play the role of invariants of quadratic nonlinearity for the diatomic case, as they inform the construction of inverse problems for the determination of the nonlinear parameters in diatomic granular chains with arbitrary constitutive characteristics.

We move then into the strongly nonlinear regime by considering the wave response of granular chains and crystals that are either subjected to moderate precompression or experience large amplitudes of excitation. In this regime, in addition to the envelope modulation, the effects of nonlinearity manifest in the formation of higher order harmonics. These harmonics are allowed to propagate in the crystal as long as a branch of the dispersion relation is available in their interval of frequency. In the case of a diatomic chain, we observe that, by exciting the structure at a frequency lying in the acoustic mode

band, if the nonlinearity is strong, we can activate second harmonics that live on the optical mode and travel according to the phononic characteristics of such mode. By means of this mode hopping mechanism, we can apply an excitation with certain spectral and modal characteristics and observe two distinct response features, one with the characteristics of the input, the other with those of the branch of the dispersion relation that has been engaged by the higher harmonic.

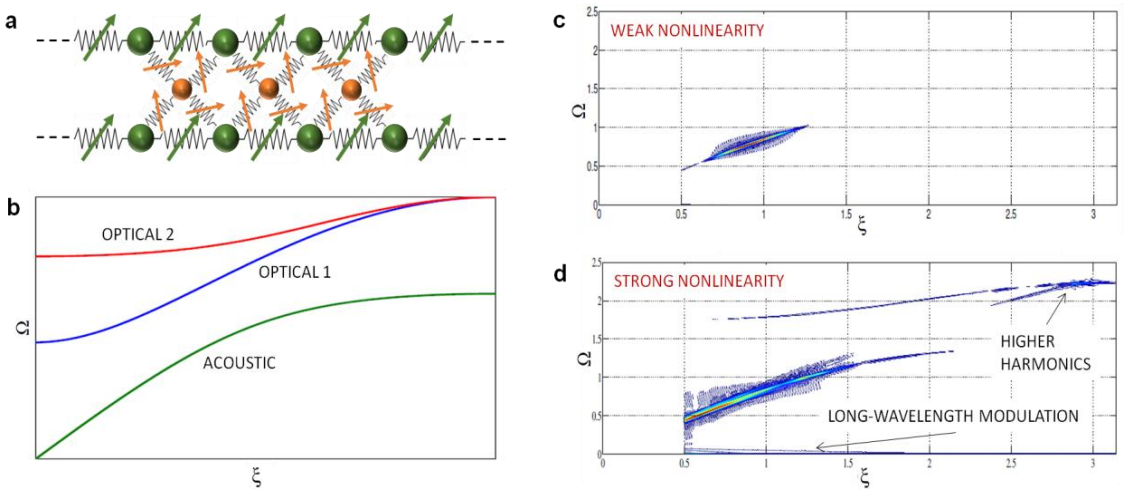

Figure 1 - Mode hopping in 1.5-D nonlinear diatomic crystal structure with cross links. a) Lattice topology. b) Band diagram of corresponding linear lattice featuring forward propagating optical modes. c-d) Spectrum of response to excitation with carrier frequency prescribed in the acoustic band: in the presence of strong nonlinearity (high amplitudes of excitation) mode hopping is observed as the higher harmonics activate the optical modes.

This concept can be fully appreciated by considering more complex nonlinear lattice topologies, such as the one shown in Fig.1a, which corresponds to a 1.5-dimensional crystal with cross links. As shown in Fig.1b, the band structure features three modes, the acoustic mode and two optical modes, both with forward-going wave characteristics. Let us assume to excite the crystal at one end with an excitation with frequency falling within the acoustic branch. If the amplitude of excitation is small, we operate in a weakly nonlinear regime and the response consists of the sole acoustic mode, as shown in Fig.1c. On the contrary, if we increase the amplitude of excitation to trigger strong nonlinearity conditions, we now simultaneously activate all three modes, as visible from the rich response signature in the spectral plane of Fig.1d. As the modes are associated with different mode shapes, i.e., different intra-cell motion between particles, the wave propagates in the physical space as the superposition of different deformation mechanisms, which contributes to the overall packet distortion. All the propagating modes display the long-wavelength modulation characteristics that have been linked to the effects of equivalent quadratic nonlinearity.

The mode hopping effect opens up opportunities for the design of nonlinear metamaterials with tunable and switchable functionalities, in which the regime of nonlinearity, which can be externally controlled through the amplitude of excitation, determines the modal characteristics of the observed wavefield. This can lead to the design of devices such as amplitude filters and amplitude switches.

References

G. Huang, Z.-P. Shi, Z. Xu, Asymmetric intrinsic localized modes in a homogeneous lattice with cubic and quartic anharmonicity, *Physical Review B*, **47** [21], 561-564, [1993]

R. Ganesh, S. Gonella, Spectro-spatial wave features as detectors and classifiers of nonlinearity in periodic chains, *Wave Motion*, **50** [4], 821-835, [2013]

Microscale Granular Acoustic Metamaterials

Nicholas Boechler[1]

[1] *Department of Mechanical Engineering, University of Washington, Seattle, WA*
boechler@uw.edu

Locally-resonant acoustic metamaterials and ordered granular media both have been shown to drastically affect acoustic wave propagation. In each case, this stems from the ability to tailor the dispersive characteristics of the material, and in the case of granular media, a response which is tunable from linear to highly nonlinear regimes that originates from the Hertzian relationship between elastic particles in contact. Locally-resonant acoustic metamaterials have been shown to support an array of non-naturally occurring properties, including negative effective density, modulus, index, and have been suggested for applications such as superlenses and invisibility cloaks, all of which are based upon linear dynamical phenomena. Alternatively, through a combination of periodicity induced dispersion and nonlinearity, ordered granular media have been shown to support unique phenomena[1] including nonlinear intrinsic localized modes, (such as solitary waves and discrete breathers), tunable band gaps, frequency conversion, and non-reciprocity. However, there remains one major current limitation. Ordered granular media are typically large (mm–cm particle dimensions) and tend to function at sonic frequencies (less than 20 kHz). Reducing the particle size to the microscale decreases the overall system size and increases the characteristic frequencies of the system into the MHz–GHz range, typical of applications such as RF signal processing and biomedical ultrasound. In addition to new potential applications, this scalability is not trivial as the dominant physics governing microscale particle contact is different than for macroscopic particles. For instance, adhesion is nearly negligible at macroscopic scales but becomes significant at micron scales, affecting the contact-based interaction between particles. Furthermore, factors such as surface roughness and capillary bridges are expected to play a more significant role.

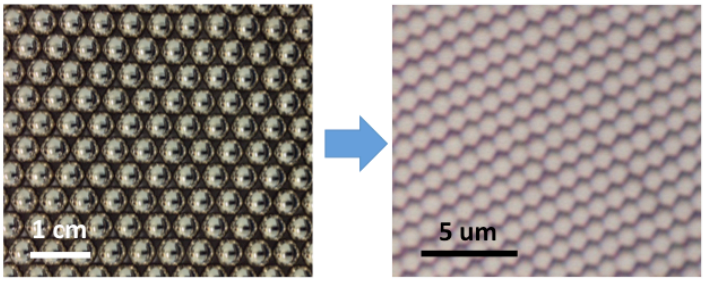

Figure 1: Macroscale to microscale ordered granular media.

For this symposium, I will discuss my recent collaborative work[2], in which we studied a locally-resonant metamaterial for surface acoustic waves (SAWs) composed of a hexagonally packed monolayer of $D = 1.08\ \mu$m diameter silica microspheres (ordered granular media) that are adhesively coupled to the surface of an aluminum coated fused silica substrate (as shown in Fig. 1). In this system, the role of the local-resonance is played by the axial contact resonance of the microspheres (as shown by the idealized model in Fig. 2). By utilizing the contact-based resonance, it is expected that a rich array of nonlinear dynamical phenomena may potentially be observed in the future as in the case of macroscale granular media, but within the context of locally-resonant metamaterials.

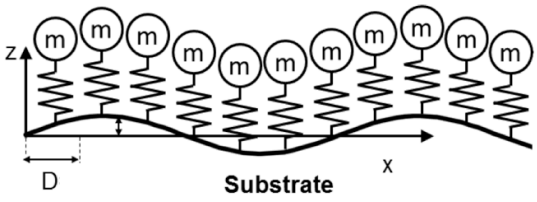

Figure 2: Model of a microsphere-based metamaterial for surface acoustic waves

The silica monolayers were assembled using the "wedge-shaped cell" convective self-assembly technique. A laser-based transient grating technique was used to generate SAWs in the coupled system and measure their dispersion. In summary, two laser pulses are crossed at the aluminum surface of the sample, and interfere to form a periodic intensity pattern. Absorption of the laser light by the alumi-

num induces a rapid thermal expansion, which launches counter-propagating SAWs with a wavelength defined by the period of the optical interference pattern. By changing the crossing angle of the beams, the wavelength of the induced SAW is varied. The temporal response of the propagating SAWs is measured with a probe beam that is diffracted off the SAWs, interfered with a reference beam, and directed to a photodiode. The Fourier spectra of the measured signals, as a function of SAW wavelength, is shown in Fig. 3. The markers correspond to identified frequency peaks. The measured dispersion shows "avoided crossing" phenomena as a result of the hybridization of the contact resonance of the microspheres with the SAWs in the substrate. Such avoided crossing phenomena is characteristic of a metamaterial with negative effective mass density induced by a dipole-like resonance. We match our measured dispersion using a simple model based on the schematic shown in Fig. 1, using only the contact resonance frequency as the single fitting parameter, and find excellent agreement. We compare the fitted contact resonance frequency with estimates based upon the Derjaguin-Muller-Toporov (DMT) contact model.

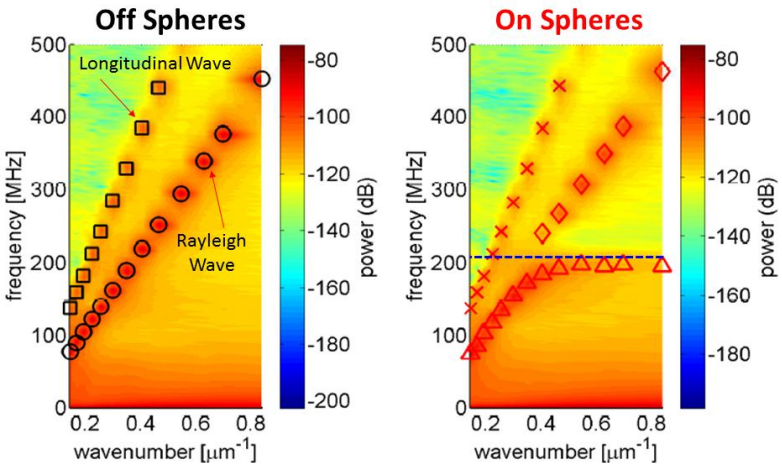

Figure 3: Measured dispersion for substrate regions without (left) and with (right) a coupled microsphere monolayer.

This work has direct application to the study of micro- and nanoparticle contact mechanics and enables a new class of locally-resonant metamaterial for SAWs. More generally, this study opens the door for future investigations of new types ordered micro- and nanoscale granular materials and possible nonlinear dynamical phenomena occurring therein. As part of this symposium presentation, I will also discuss our group's recent progress, including nonlinear discrete element modeling efforts, and give an overview my future vision pertaining to this work.

References

[1] G. Theocharis, N. Boechler, and C. Daraio, Ch. 6 of *Acoustic Metamaterials and Phononic Crystals*, edited by P. Deymier, Springer-Verlag Berlin Heidelberg, 217-251 [2013]
[2] N. Boechler, J. K. Eliason, A. Kumar, A. A. Maznev, K. A. Nelson, and N. Fang, *Phys. Rev. Lett.*, **111**, 036103 [2013]

PHONON TRANSPORT IN PERIODIC MATERIALS WITH FEATURE SIZES OF 1 nm to 1 μm

Alan J. H. McGaughey

Department of Mechanical Engineering, Carnegie Mellon University, Pittsburgh PA, 15213
mcgaughey@cmu.edu

Abstract: Two periodic materials are investigated: (i) superlattices that have period lengths on the order of phonon wavelengths, and (ii) porous films with pore spacings on the order of phonon mean free paths. The interplay between these three length scales is used to explain thermal conductivity trends predicted from molecular dynamics simulations, lattice dynamics calculations, and the Boltzmann transport equation.

The nature of phonon transport in a periodic material depends on the relative magnitudes of the phonon wavelengths, the phonon mean free paths, and the characteristic dimensions of the periodicity. Atomistic and mesoscale simulations provide an opportunity for studying the interplay between these length scales.

Superlattices with period lengths of 1 to 10 nm will first be considered. This dimension range is comparable to the phonon wavelengths that contribute to thermal transport. The particular focus is how species mixing at the interfaces affects the cross-plane thermal conductivity and the properties of individual phonon modes.

As shown in Fig. 1, for a silicon-germanium superlattice modeled in molecular dynamics simulations, the introduction of 12% species mixing in the monolayers closest to the interfaces changes the magnitude of thermal conductivity and the period length trend.[1] The effect is most pronounced for a period of 2.5 nm, where the thermal conductivity decreases by an order of magnitude. These changes are due to the elimination of phonons that exist based on the periodicity of the superlattice (i.e., so-called "coherent" phonons) by the interfacial mixing.

To further investigate the effect of interfacial mixing, a series of superlattices modeled using the Lennard-Jones potential are next studied using molecular dynamics simulations and lattice dynamics calculations.[2] The predicted phonon lifetimes for superlattices with perfect and mixed interfaces are plotted in Fig. 2 as a function of phonon frequency. While the mixing does not affect the low-frequency (i.e., long-wavelength) phonon modes, the magnitudes and trends of higher frequency modes are noticeably changed, particularly for shorter-period superlattices.

Silicon thin films with a periodic arrangement of unfilled cylindrical pores present an opportunity to study a system where the characteristics dimensions of the periodicity range from 100 nm to 1 μm. These dimensions are much greater than the phonon wavelengths but comparable to the phonon mean free paths. Due to the large length scales of the periodicity, a full atomistic treatment is not possible. Instead, bulk phonon properties predicted from first principles calculations and a phonon free path sampling approach[3] are used to predict thermal conductivity.[4] In doing so, coherent phonons are not included in the calculations. As shown in Fig. 3, the thermal conductivity predictions are in excellent agreement with experimental measurements,[5] indicating that coherent phonons do not make a significant contribution to thermal conductivity in these structures. The periodicity does not affect the thermal transport other than providing locations for phonon-boundary scattering.

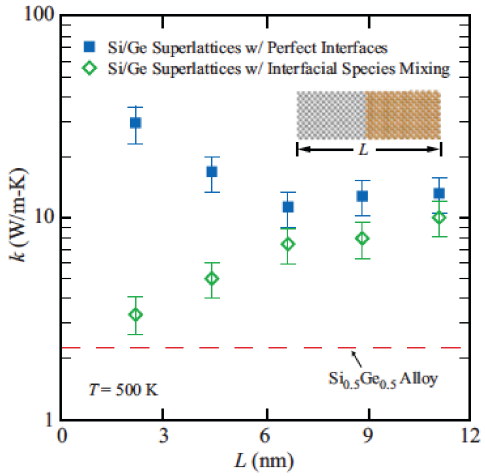

Fig. 1. Thermal conductivity of Si/Ge superlattices with perfect and mixed interfaces.[1]

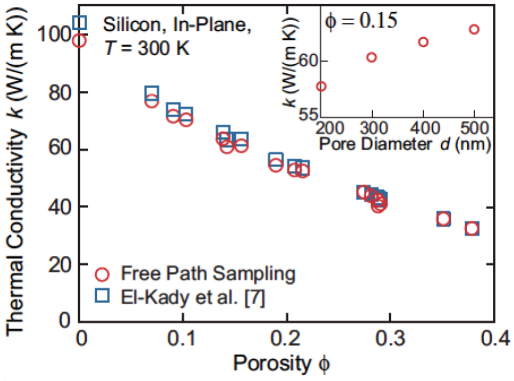

Fig. 3. Thermal conductivity of porous silicon films from modeling and experiment.[4]

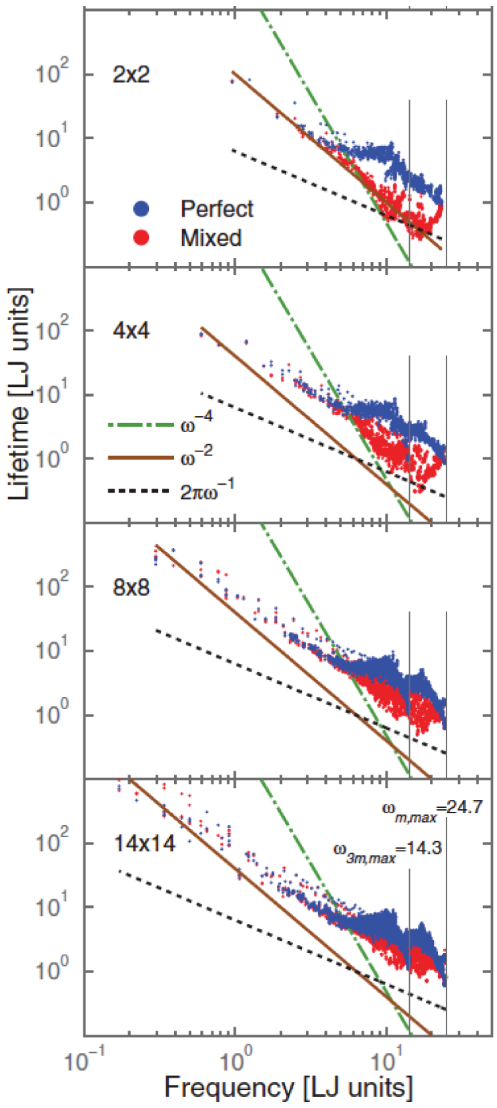

Fig. 2. Phonon lifetimes in Lennard-Jones superlattices with perfect and mixed interfaces.[2]

References

[1] E. S. Landry and A. J. H. McGaughey, *Physical Review B*, **79**, 075316 (2009).
[2] S. C. Huberman, J. M. Larkin, A. J. H. McGaughey, and C. H. Amon, *Physical Review B*, **88**, 155311 (2013).
[3] A. J. H. McGaughey and A. Jain, *Applied Physics Letters*, **100**, 061911 (2012).
[4] A. Jain, Y.-J. Yu, and A. J. H. McGaughey, *Physical Review B*, **87**, 195301 (2013).
[5] I. El-Kady, R. H. Olsson III, P. E. Hopkins, Z. C. Lessman, D. F. Goettler, B. Kim, C. M. Reinke, and M. F. Su, Progress Report SAND2012-0127, Sandia National Laboratories, California, CA (201

Thermal Transport in Micro-Scale Phononic Crystals: Observation of Coherent Phonon Scattering at Room Temperature and its implications to Thermoelectrics

Seyedhamidreza Alaie[1], Drew F. Goettler[1], Mehmet Su[1,2], Zayd C. Leseman[1,2]
Charles M. Reinke[1,3] and Ihab El-Kady[1,2,3]
[1] Mechanical Engineering Dept., University of New Mexico, Albuquerque, NM, USA
[2]Electrical and Computer Engineering Dept., University of New Mexico, Albuquerque, NM, USA
[3]Dept. of Applied Photonic Microsystems, Sandia National Laboratories, Albuquerque, NM, USA ,
ielkady@sandia.gov

Abstract: We report on the experimental observation of coherent phonon boundary scattering in micro-scale phononic crystals (PnCs) at room temperature. We show that the neglecting coherent boundary scattering leads to gross overestimation of the measured thermal conductivities of the PnC samples. We introduce a hybrid model that accounts for partial coherent and partial incoherent phonon boundary scattering. Excellent agreement with the experiment is achieved.

Almost all physical processes produce heat as a byproduct making thermoelectric (TE) systems very attractive for energy scavenging applications. Energy conversion in TE devices is based on the so called Peltier effect[1]. Here the temperature gradient resulting from expelled heat is used to force electronic transport resulting in an electric current. As such, heat transported via phonons represents a leakage mechanism and serves to reduce the efficiency of TE systems. Indeed the inability to suppress or eliminate the relative phonon contribution to thermal transport as compared to the electronic one has hindered the development of efficient TE devices. Recently, it has been proposed that coherent boundary scattering in micro-scale phononic crystals (PnCs) may hold the key to solving this problem by scattering phonons with minimal influence on electrons[2-4]. PnCs are artificial structures with a periodic variation in mechanical impedance brought about by the introduction of holes or plugs of one material into a homogenous matrix of another[5-8]. This periodic variation results in rich phonon dispersion with unusual behaviors [9]. In this communication, we focus on micro-scale PnCs formed by the introduction of air holes in a Si matrix with minimum feature sizes ≥100nm. As a phonon population traverses such a lattice, it can undergo two types of scattering processes: simple incoherent scattering as a result of encountering a boundary; and coherent Bragg-like[7] scattering due to the periodic topology of the artificial lattice of air holes. In the first type, it is assumed that the phonons will retain no phase information after each scattering event. This implies that the phonon dispersion remains unaltered due to the introduction of the air-holes. In the second type, on the other hand, it is assumed that the phase is preserved throughout several scattering events thus enabling coherent interference to occur. Consequently, this would imply a modified phonon dispersion that is sensitive to the topology of the PnC air-hole lattice. Practically, this can have profound implications because: while incoherent boundary scattering depends only on the shape, size, and separation of the holes; coherent boundary scattering additionally depends on the symmetry and topology by which these holes are distributed. Thus, the existence of coherent scattering would allow one to further reduce the thermal conductivity of the underlying material without the need for additional boundaries (e.g. more air-holes) by simply altering the PnC topology.

The claim of coherent phonon scattering in micro-scale Si/Air PnCs at room temperature has generated widespread controversy in the literature given the relatively small wavelength characteristic of the phonon population dominating the thermal transport[3,10-14]. Experimentally however, the thermal conductivity (κ) of PnC samples have consistently been measured to be significantly lower than that of an unpatterned film[2,4,11,13,14]. In fact far lower than what would be expected due to the combination of material removal and simple incoherent boundary scattering[2,4,13], thereby suggesting that another κ reduction mechanism, possibly coherent scattering, must be taking place. The controversy was heightened by the discovery that ~50% of κ in Si is carried by phonons with mean free paths (MFPs) from 100nm up to 1μm15, which was recently verified experimentally[16]. Since it is logical to assume that a

phonon remains coherent over its MFP, we suggest here that the MFP, rather than wavelength, should be used when judging whether or not coherent scattering events can take place. In which case, a large enough fraction of the phonon population could travel sufficient distances to experience the PnC lattice periodicity and thus undergo coherent scattering.

We report on the experimental observation of coherent phonon boundary scattering in micro-scale phononic crystals (PnCs) at room temperature. We investigate the existence of coherent phonon boundary scattering resulting from the periodic topology of the PnCs and its influence on the thermal in silicon. To delaminate incoherent from coherent boundary scattering, PnCs with a fixed minimum feature size, differing only in the unit cell topologies, were fabricated. A suspended island platform was used to measure the thermal conductivity. We show that the neglecting coherent boundary scattering leads to gross overestimation of the measured thermal conductivities of the PnC samples. We introduce a hybrid model that accounts for partial coherent and partial incoherent phonon boundary scattering. Excellent agreement with the experiment is achieved emphasizing the influence of coherent zone folding in PnCs. Our results yield conclusive evidence that significant room temperature coherent phonon boundary scattering does indeed take place.

References

[1] Slack, G. A. CRC Handbook of Thermoelectrics. (CRC Press, 1995).
[2]Hopkins, P. E. et al. Reduction in the Thermal Conductivity of Single Crystalline Silicon by Phononic Crystal Patterning. Nano Lett **11**, 107-112, doi:Doi 10.1021/Nl102918q (2011).
[3] Reinke, C. M. et al. Thermal conductivity prediction of nanoscale phononic crystal slabs using a hybrid lattice dynamics-continuum mechanics technique. AIP Advances **1**, 041403-041414 (2011).
[4] Yu, J.-K., Mitrovic, S., Tham, D., Varghese, J. & Heath, J. R. Reduction of thermal conductivity in phononic nanomesh structures. Nature Nanotechnology, **5**, 718-721, (2010).
[5] Reinke, C. M., Su, M. F., Olsson, R. H. & El-Kady, I. Realization of optimal bandgaps in solid-solid, solid-air, and hybrid solid-air-solid phononic crystal slabs. Appl Phys Lett **98**, doi:Artn 061912
Doi 10.1063/1.3543848 (2011).
[6] Su, M. F., Olsson, R. H., Leseman, Z. C. & El-Kady, I. Realization of a phononic crystal operating at gigahertz frequencies. Appl Phys Lett **96**, 053111 (053113 pp.), doi:10.1063/1.3280376 (2010).
[7] Olsson, R. H., III et al. in IEEE International Ultrasonics Symposium. 1150-1153.
[8] El-Kady, I., Olsson, R. H., III & Fleming, J. G. Phononic band-gap crystals for radio frequency communications. Appl Phys Lett **92**, 233504-233501-233503, doi:10.1063/1.2938863 (2008).
[9] Kushwaha, M. S., Halevi, P., Dobrzynski, L. & Djafari-Rouhani, B. Acoustic band structure of periodic elastic composites. Physical Review Letters **71**, 2022-2025 (1993).
[10] Hao, Q., Chen, G. & Jeng, M.-S. Frequency-dependent Monte Carlo simulations of phonon transport in two-dimensional porous silicon with aligned pores. Journal of Applied Physics **106**, 114321-114310 (2009).
[11] Tang, J. et al. Holey Silicon as an Efficient Thermoelectric Material. Nano Lett **10**, 4279-4283, doi:10.1021/nl102931z (2010).
[12] Jain, A., Yu, Y.-J. & McGaughey, A. J. H. Phonon transport in periodic silicon nanoporous films with feature sizes greater than 100 nm. Physical Review B **87**, 195301 (2013).
[13] Bongsang, K. et al. in Micro Electro Mechanical Systems (MEMS), 2012 IEEE 25th International Conference on 176-179 (2012).
[14] El-Kady, I. et al. Phonon Manipulation with Phononic Crystals. (Sandia National Laboratories, 2012).
[15] Esfarjani, K., Chen, G. & Stokes, H. T. Heat transport in silicon from first-principles calculations. Physical Review B **84**, 085204 (2011).

Nanophononic Metamaterial: Slowing Down Heat Transfer by Mechanical Vibrations

Bruce L. Davis, Mahmoud I. Hussein[1]

[1] *Department of Aerospace Engineering Sciences, University of Colorado Boulder, Boulder, CO 80309*
mih@colorado.edu

Abstract: We present the concept of a locally resonant nanophononic metamaterial for thermoelectric energy conversion. Considering a silicon thin-film with a periodic array of pillars extruding off the free surfaces, we show that the coupling of the local vibration modes of the pillars with the travelling wave modes of the underlying thin-film atomic lattice leads to a significant reduction in the thermal conductivity. The proposed concept provides a new paradigm for high-performance, scalable thermoelectric materials and a new perspective on the definition of a metamaterial.

Engineered manipulation of phonons can yield beneficial thermal properties in semiconducting materials.[1,2] One pivotal application relates to thermoelectric materials, or the concept of converting energy in the form of heat into electricity and vice-versa. The ability to use nanostructuring to reduce the thermal conductivity without negatively impacting the power factor provides a promising avenue for achieving high values of the thermoelectric energy conversion figure-of-merit, *ZT*. In this work, we propose a new strategy for the manipulation of phonon transport that seeks to achieve this goal. Termed "nanophononic metamaterial," we consider a configuration consisting of a thin-film with a periodic array of pillars erected on one or two of the free surfaces.[3] The pillars qualitatively alter the base thin-film phonon spectrum due to a hybridization mechanism between their local resonances and the underlying atomic lattice dispersion. Using an experimentally-fitted lattice-dynamics-based model using silicon as a base material, we conservatively predict a drop in the thermal conductivity to as low as 50% of the corresponding uniform thin-film value. It is noteworthy that this drop is realized despite the fact that the pillars add more phonon modes to the spectrum (see Fig. 1).

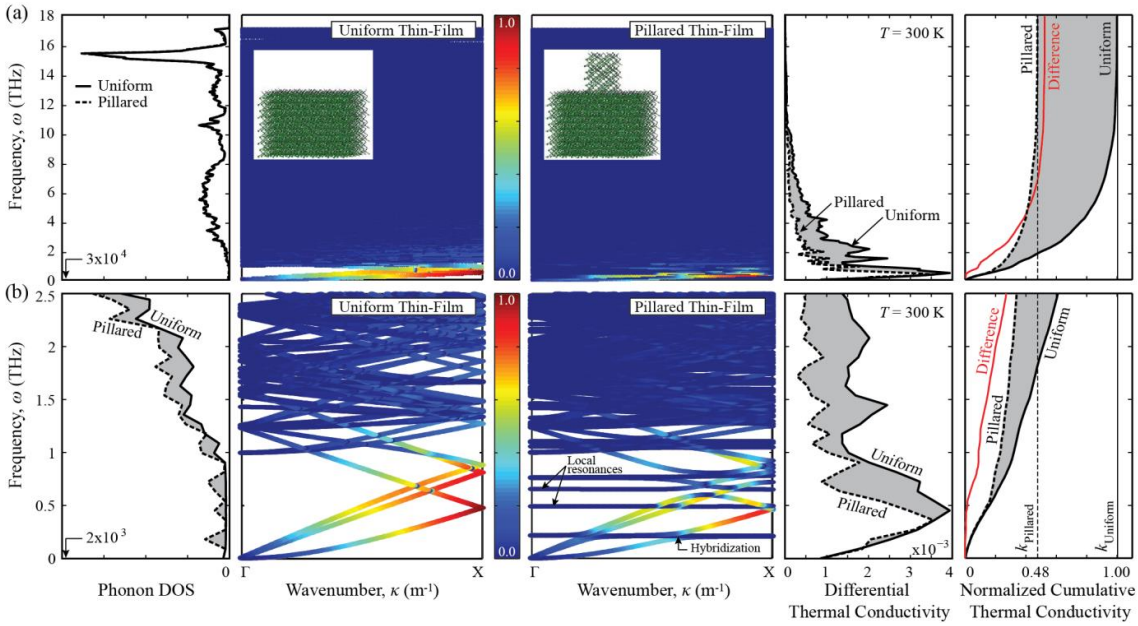

Figure 1. Comparison of the phonon dispersion and thermal conductivity of a pillared silicon thin film with a corresponding uniform thin film. The dispersion curves are colored to represent the modal contribution to the cumulative thermal conductivity, normalized with respect to the highest modal contribution in either configuration. The full spectrum is shown in (a) and the $0 \leq \omega \leq 2.5$ THz portion is shown in (b). Phonon DOS and the thermal conductivity, in both differential and cumulative forms, are also shown. The gray regions represent the difference in quantity of interest between the two configurations and illustrate the remarkable effects of the pillars.

From the point of view of thermoelectric materials, the advantages that the presented concept/configuration provide include: (1) powerful mechanism for thermal conductivity reduction since this is done by reducing group velocities for a large number of phonons across the entire spectrum (as opposed to only a narrow frequency window), (2) favourable attributes for thermoelectric energy conversion since no scatterers are utilized within the main body of the thin film, thus reducing the likelihood of electron scattering, (3) insensitivity to geometrical tolerances due to the nature of localized vibration modes, (4) favourable properties are derived from the inherent nanostructural dynamics as opposed to the intrinsic properties of the semiconducting material used, thus allowing for a flexibility in the choice of the base material, and (5) scalable configuration that can be easily integrated into devices.

From the point of the theory of metamaterials, this work demonstrates that favourable "meta" properties may stem from dynamical behaviour spanning the entire spectrum as opposed to only the subwavelength regime as is currently considered in electromagnetic[4,5] and acoustic metamaterials.[6] Furthermore, the unusual properties that arise are apparent without the need to resorting to an effective medium description. These two attributes provide a broader perspective on the definition of a locally resonant metamaterial.

References

[1] A. A. Balandin and K. L. Wang, *Phys. Rev. B* **58**, 1544 (1998).
[2] G. Chen, *Int. J. Therm. Sci.* **39**, 471 (2000).
[3] B. L. Davis and M. I. Hussein, *Phys. Rev. Lett.* **112**, 055505 (2014).
[4] J. B. Pendry, A. J. Holden, D. J. Robbins and W. J. Stewart, *IEEE Trans. Microwave Theory* **47**, 2075 (1999).
[5] D. R. Smith, W. J. Padilla, D. C. Vier, S. C. Nemat-Nasser and S. Schultz, *Phys. Rev. Lett.* **84**, 4184 (2000).
[6] Z. Y. Liu, X. X. Zhang, Y. W. Mao, Y. Y. Zhu, Z. Y. Yang, C. T. Chan and P. Sheng, *Science* **289**, 1734 (2000).

PHONONIC CRYSTAL SUPPORTING FERMION-LIKE ROTATIONAL MODES

Pierre A. Deymier[1], **Keith Runge**[1], **Nicklas Swinteck**[1]

[1] *Department of Materials Science and Engineering, University of Arizona, Tucson AZ 85721*
deymier@email.arizona.edu; krunge@email.arizona.edu; swinteck@email.arizona.edu

Abstract: We investigate rotational modes in a phononic crystal composed of stiff polymer inclusions in a soft elastomer matrix. We show the existence near the Γ point of modes where the inclusions and the matrix regions between inclusions rotate in phase and out of phase. These modes are investigated within a model that parallels the Dirac formalism for relativistic quantum particles. This formalism, in which modes have both a spinor and a spatio-temporal part, clearly exposes fermion-like behavior for some in-phase rotational modes.

Phononic crystals (PC) comprised of periodically arranged elastic scatterers of one material dispersed periodically throughout a different homogeneous matrix material can support rotational modes[1-7]. Sainidou et al.[4] and Zhao et al.[5] revealed theoretically that rotary resonance modes can strongly interact with Bragg gaps to yield extremely wide absolute acoustic band gaps. Peng et al.[7] proposed a one-dimensional lumped model composed of finite-sized masses and mass-less springs to provide an understanding of the underlying physics behind rotary resonance in two-dimensional (2D) solid/solid PCs. Several studies have characterized rotational elastic waves in three-dimensional (3D) granular structures comprised of pre-compressed, regular arrangements of spherical elastic particles[8-10]. We consider a PC composed of a square array of polystyrene (PS) cylinders with square cross section embedded in a homogeneous, elastic matrix of polydimethylsiloxane (PDMS). This combination of materials with sharp contrast in the transverse speed of sound offers distinctive elastic band structures with modes corresponding to rotational waves.

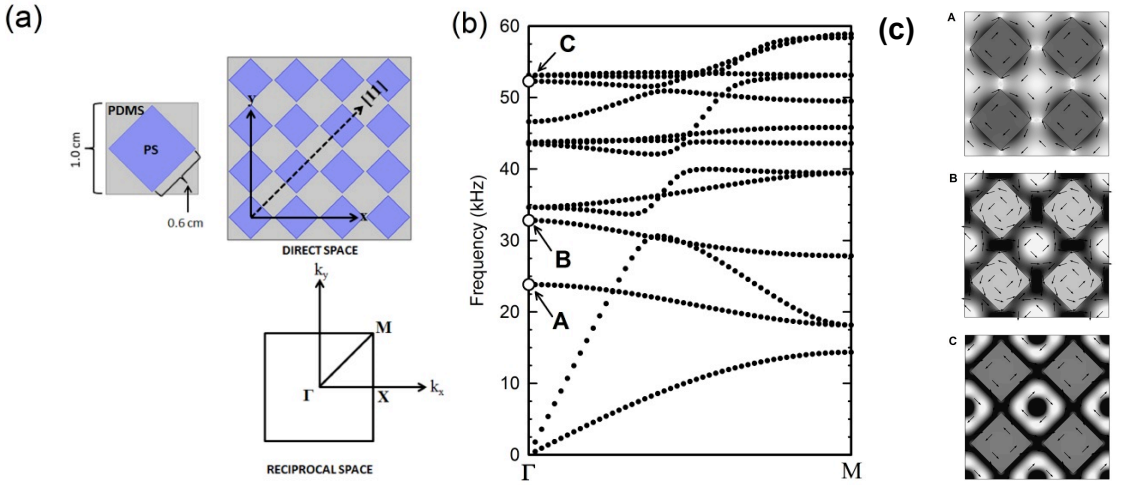

Figure 1: (a) Schematic illustration of the PS/PDMS PC; (b) Calculated band structure along the ΓM direction. Three rotational modes are marked as A,B, and C; (c) Displacement fiel associated with modes A, B, and C. The elastic parameters for PS and PDMS are as follows: ρ_{PS} = 1050 kg/m^3, $C_{L,PS}$ = 2350 m/s, $C_{T,PS}$ = 1230 m/s, ρ_{PDMS} = 965 kg/m^3, $C_{L,PDMS}$ = 1100 m/s and $C_{T,PDMS}$ = 200 m/s, where ρ, C_L and C_T denote density, longitudinal speed of sound and transverse speed of sound, respectively. The lattice constant of the PC is a = 1cm. The length of the edge of the square inclusion is 0.6 cm for a filling fraction ff = 0.36.

Mode A and C in Fig. 1 shows alternating regions of PS and PDMS rotating out of phase. In contrast, in the case of mode B, the PS and PDMS regions are rotating in phase. This mode is uniquely enabled by the very low value of the transverse speed of sound in the PDMS. To elucidate the nature of the observed rotational modes we consider a 1D block-spring model that can reproduce the dispersion relation associated with rotational mode B of the 2D PC (see Fig. 2).

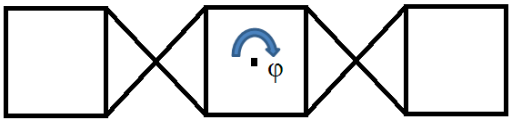

Figure 2: Schematic illustration of 1D block (square)-spring (diagonal lines) mechanical model that can support rotational waves. Φ refers to the rotational degree of freedom of the blocks.

In the long wavelength limit, the equation of motion for the angular variable, φ, takes the form:

$$\frac{\partial^2 \varphi}{\partial t^2} - \beta^2 \frac{\partial^2 \varphi}{\partial x^2} + \alpha^2 \varphi = 0 \tag{1}$$

α and β are parameters related to the stiffness or the springs and the geometry of the 1D model. Equation (1) is isomorphic to the Klein-Gordon equation for relativistic quantum particles. It involves second derivatives with respect to continuous time and position of the angular degree of freedom. Following the approach of Dirac in linearizing the Klein-Gordon equation, we obtain a wave equation in terms of first order spatial and temporal derivatives.

$$\left[\boldsymbol{\sigma}_x \frac{\partial}{\partial t} + i\beta \boldsymbol{\sigma}_y \frac{\partial}{\partial x} \pm i\alpha \boldsymbol{I}\right] \psi = 0 \tag{2}$$

where $\boldsymbol{\sigma}_x$ and $\boldsymbol{\sigma}_y$ are the 2x2 Pauli matrices: $\begin{pmatrix} 0 & 1 \\ 1 & 0 \end{pmatrix}$ and $\begin{pmatrix} 0 & -i \\ i & 0 \end{pmatrix}$, respectively. In equation (2), the $\pm$ correspond to the "particle" and "antiparticle" solutions of Dirac equation. The wave function solution of the Dirac-like equation can be written in the general form $\psi(\omega, k) = \xi(k)\phi(\omega, k)$ where $\xi(k)$ is the spinor part and $\phi(\omega, k)$ is the spatio-temporal part of the wave function which can be written as a plane wave, $\phi(\omega, k) = e^{-i\omega t} e^{ikx}$. $\xi(k)$ is a two component spinor. The Eigen values are given by $\omega = \pm\sqrt{\alpha^2 + \beta^2 k^2}$ and the two-spinor corresponding to the positive branch, ω>0, takes the form (a similar solution is obtained for ω<0 but with alternating signs):

$$\xi(k) = a_0 \begin{pmatrix} -\sqrt{\omega - \beta k} \\ +\sqrt{\omega + \beta k} \end{pmatrix} \tag{3}$$

The spinor part of the rotational wave function is related to the coupling between the senses of wave propagation. By calculating observables associated with operators that operate only on the spinor part of the wave function, for the superposition of two waves, we can identify conditions that constrain Eigen states of the system. In particular, we have identified conditions that impose the lifting of the frequency degeneracy at the origin of the Brillouin zone as is the case for mode B in the band structure of the 2D PC. This observation suggests that rotational modes in PC may possess fermion-like (or spinor-related) characteristics which effects can be observed in their band structure. The fermion-like behavior that we characterized lifts the degeneracy between bands with positive negative frequency at the origin of the Brillouin zone. Finally, the methods of Quantum Field Theory can be applied to this model. In particular, one can write the Lagrangians and the corresponding Hamiltonians that generate equations (2). Introducing field operators as well as amplitude operators in place of a_0, the condition of positive energy leads to the requirement that the amplitude operator anticommutes, a characteristics of Fermion-like behavior.

Conical Dirac dispersions or Dirac-like behavior in PC[11] has been observed and can lead to zero refractive index. However, the fermion-like behavior of rotational waves reported here opens up opportunities in the control of the phase of elastic waves.

References

[1] F. Liu, Y. Lai, X. Huang and C. T. Chan, Phys. Rev. B 84, 224113 (2011).
[2] G. Wang, X. Wen, J. Wen, L. Shao and Y. Liu, Phys. Rev. Lett. 93, 154302 (2004).
[3] Y. Lai, Y. Wu, P. Sheng and Z. Q. Zhang, Nat. Mater. 10, 620 (2011).
[4] R. Sainidou, N. Stefanou and A. Modinos, Phys. Rev. B 66, 212301 (2002).
[5] H. Zhao, Y. Liu, G. Wang, J. Wen, D. Yu, X. Han and X. Wen, Phys. Rev. B 72, 012301 (2005).
[6] K. Maslov, V. K. Kinra and B. K. Henderson, Mech. Mater. 31, 175 (1999).
[7] P. Peng, J. Mei and Y. Wu, Phys. Rev. B 86, 134304 (2012).
[8] A. Merkel, V. Tournat and V. Gusev, Phys. Rev E 82, 031305 (2010).
[9] V. Tournat, I. Pérez-Arjona, A. Merkel, V. Sanchez-Morcillo and V. Gusev, New J. Phys. 13, 073042 (2011).
[10] A. Merkel, V. Tournat and V. Gusev, Phys. Rev. Lett. 107, 225502 (2011).
[11] J. Mei, Y. Wu, C.T. Chan, and Z.-Q. Zhang, Phys. Rev. B 86, 035141 (2012)

Amplitude-Dependent Wave Devices Based on Nonlinear Periodic Materials

Massimo Ruzzene[1], Michael J. Leamy[2]

[1] School of Aerospace Engineering, Georgia Institute of Technology,
[2] School of Mechanical Engineering, Georgia Institute of Technology,
michael.leamy@me.gatech.edu

Abstract: This talk will discuss recent progress on analytical, computational, and experimental analysis of nonlinear acoustic metamaterials. The inclusion of nonlinear elements in periodic unit cells allows for amplitude-dependent tuning of acoustic band structure. This enables, for example, tunable bandgaps, waveguides, filters, resonators, and logic elements (diodes, multiplexors, etc.). In order to elucidate this advantageous behavior, a series of perturbation techniques have been developed for predicting amplitude-dependent dispersion and group velocity characteristics in weakly-nonlinear discrete and continuous systems. Analysis of wave-wave interactions reveals, for example, the manner in which a 'control wave' can alter the dispersion of a 'primary wave,' modifying its group velocity and spatial beaming behavior. This and other novel nonlinear behavior will be discussed using results from analytical, computational, and experimental studies.

Theoretical Background

We consider dispersion shifts for an infinite chain of Duffing oscillators coupled by a weak stiffness nonlinearity (see Fig. 1):

$$m\ddot{u}_p + k_1(2u_p - u_{p+1} - u_{p-1}) + \varepsilon k_1(u_p - u_{p+1})^3 + \varepsilon k_1(u_p - u_{p-1})^3 = 0 \qquad (1)$$

where $u_p(t)$ denotes displacement from equilibrium of the *p*th degree of freedom, *m* denotes mass, ε denotes a small perturbation parameter, and k_1 and k_3 denote linear and nonlinear stiffness coefficients, respectively.

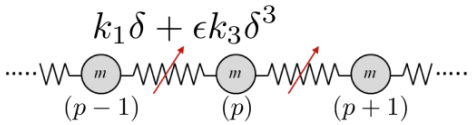

Figure 1: Nonlinear spring mass chain with cubic nonlinear interaction (δ denotes the relative displacement of neighboring masses).

When this system is linear (i.e., $\varepsilon = 0$), the dispersion is governed by the well-known dispersion relationship $\omega(\mu) = \omega_n\sqrt{2 - 2cos\mu}$ where $\omega_n = \sqrt{k_1/m}$ and μ is the Bloch wavenumber. When $\varepsilon \neq 0$, perturbation analysis[1,2,3] provides a closed-form approximation of the amplitude-dependent nonlinear dispersion relationship,

$$\omega(\mu) = \omega_n\sqrt{2 - 2cos\mu} + \varepsilon\frac{3}{8}\frac{k_3A^2}{m\omega_n}(2 - 2cos\mu)^{3/2} + O(\varepsilon^2)\,, \qquad (2)$$

where *A* is the amplitude of free wave propagation and the dispersion correction term \$ $\varepsilon\frac{3}{8}\frac{k_3A^2}{m\omega_n}(2 - 2cos\mu)^{3/2}$ causes the cutoff frequency to shift upwards or downwards for hardening and softening

springs, respectively. Similar dispersion relationships can be derived for two- and three-dimensional systems, which admit solutions with amplitude-dependent group velocity[2]. Wave-wave interactions can also be considered which yield additional corrections to dispersion[3,4].

Applications

Since nonlinear periodic materials exhibit amplitude-dependent dispersion, group velocity, and bandgaps, they enable novel wave-based devices, several of which are depicted in Figs. 2 and 3. The first device uses two frequencies close to the optical and acoustic cutoffs of a nonlinear diatomic chain. By tuning the gain to be either high or low, the device can isolate each of the frequencies. This may be useful, for example, in acoustic multiplexing and demultiplexing. The second device uses a nonlinear material sandwiched between two linear materials – at small amplitude, a forcing at the center of the device propagates waves similar to a linear monatomic lattice, while at larger amplitudes the device behaves as a nonlinearly-activated waveguide.

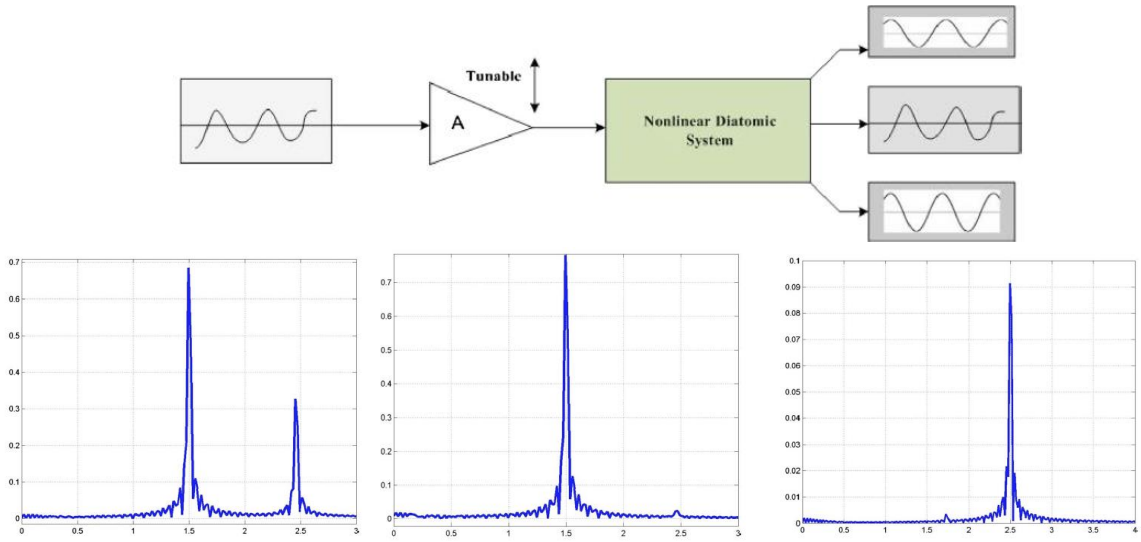

Figure 2: Amplitude-dependent frequency isolator arising from a nonlinear diatomic chain and verified by numerical simulations. Bottom subfigures show (left) the input frequencies, (center) the selection of the low frequency using a small gain, and (right) the selection of the high frequency using a large gain.

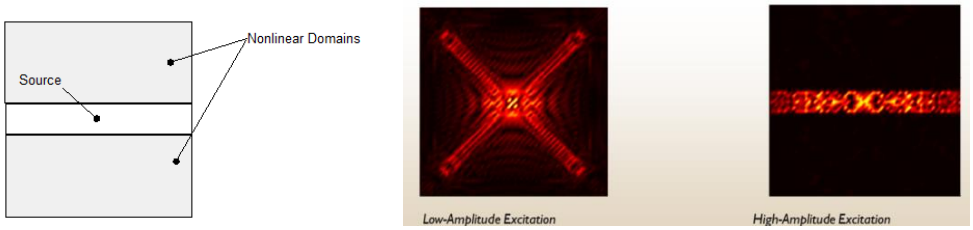

Figure 3: Nonlinearly-activated waveguide: (left) a linear material is sandwiched between two nonlinear material, (center) response at low amplitude, and (right) response at large amplitude.

References

[1] Narisetti, R.K., Leamy, M.J., Ruzzene, M., "A Perturbation Approach for Predicting Wave Propagation in One-Dimensional Nonlinear Periodic Structures," Journal of Vibration and Acoustics, **132** (3): 031001, pp. 1-11, 2010.
[2] Narisetti, R.K., Ruzzene, M., Leamy, M.J., "A Perturbation Approach for Analyzing Dispersion and Group Velocities in Two-Dimensional Nonlinear Periodic Lattices," Journal of Vibration and Acoustics, **133** (6): 061020, pp. 1-12, 2011.
[3] Manktelow, K., Leamy, M., Ruzzene, M., "Multiple Scales Analysis of Wave-Wave Interactions in a Cubically Nonlinear Monoatomic Chain," Journal of Nonlinear Dynamics, **63**: 193-203, 2011.
[4] Manktelow, K., Leamy, M., Ruzzene, M., "Nonlinear Wave Interactions in Multi-Degree of Freedom Periodic Structures," Wave Motion, in press, 2014.

Phonon Heat Management by Periodic Materials: How to Treat Heat like Sound

Martin Maldovan[1]

[1] *School of Chemical and Biomolecular Engineering, Georgia Institute of Technology*
maldovan@gatech.edu

Abstract: A new class of periodic material is introduced where heat flow is manipulated by the specular reflection of phonons. By engineering the phonon frequency spectrum, a range of phonons with large wavelengths is selected to carry the heat and matched to a phononic band gap. These periodic materials can lead to an unprecedented control of thermal energy, since heat can now be manipulated in a similar way to sound in periodic phononic band gap materials. Applications include thermoelectric and thermal protection devices.

To be able to precisely manipulate phonon heat conduction is essential in the development of many technological devices such as thermoelectrics, nano- and optoelectronics, fuel cells, solar cells, and thermal insulation/protection materials. Conventional techniques to control thermal energy flow have been based on introducing impurities, defects, and alloy atoms in the atomic lattice. In recent years, however, many alternative methods have been developed and several nanostructures and complex compounds have been employed to control phonon heat transport. Here, we introduce a new class of periodic material, called a ''thermocrystal'', that can manipulate the flow of thermal energy by exploiting the specular reflection of phonons from internal surfaces[1,2]. We show that the two-dimensional patterning of nanostructured alloys can lead to a radical new departure on thermal energy management. These periodic materials can guide heat as photonic and phononic crystals guide light and sound, respectively. They lay the foundation for a wide range of applications ranging from improved thermoelectric materials to more efficient thermal insulation/protection materials.

The propagation of phonons with sonic frequencies have been managed in the last decade by purposely-designed periodic composite structures known as phononic crystals[3]. These periodic structures can control sound in many useful ways due to the existence of forbidden frequency band gaps. Because of interference effects, phononic band gaps occur when the phonon wavelengths λ are comparable to the periodicity a of the material (i.e. Bragss's Law: $\lambda \sim 2a$). If we consider using phononic crystals to control heat conduction in semiconductors such as silicon, where thermal phonon wavelengths are $\lambda \sim 1$–10 nm, the structure periodicity should be $a \sim 2$ nm. Periodic composite materials having such a small periodicity are extremely difficult to realize in practice. To overcome this difficulty, we introduce a scheme to create a flow of thermal energy carried by phonons with specific wavelengths (heat spectrum engineering), which involves the use of alloy atoms, nanoparticles, and boundary size effects. We obtain a flow of thermal energy carried by long-wavelength phonons which is considerably reduced to the specific wavelength range that corresponds to a phononic band gap. In this manner, many applications and devices already demonstrated for sound (such as stop bands, mirrors, waveguides, cavities, etc.) can be now applied to heat conduction. Thermocrystals offer the possibility of significant new developments in the next generation of thermoelectric devices and thermal insulation/protection materials.

References

[1] M. Maldovan, "Narrow low-frequency spectrum and heat management by thermocrystals", Physical Review Letters **110**, 025902 (2013).
[2] M. Maldovan "Sound and heat revolutions in phononics", Nature **503**, 209 (2013).
[3] M. S. Kushwaha, P. Halevi, L. Dobrzynski, and B. Djafari-Rouhani, "Acoustic band structure of periodic elastic compo sites" Physical Review Letters **71**, 2022 (1993).

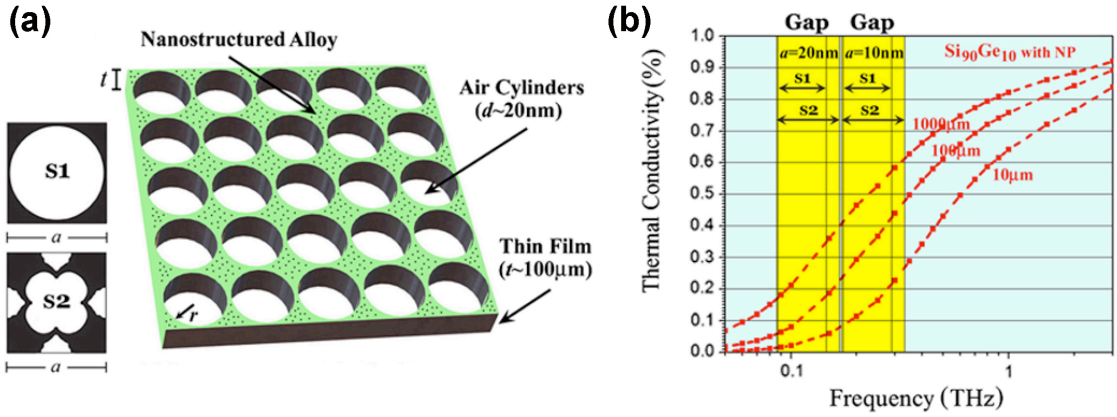

Figure 1: **Thermocrystals,** (a) A thermocrystal made of periodically arranged air cylinders in a nanostructured alloy thin film. (b) The cumulative thermal conductivity as a function of phonon frequencies for nanostructured $Si_{90}Ge_{10}$ thin films with thicknesses 10, 100, and 1000 microns (dashed lines). Highlighted vertical areas show the phononic band gap frequencies for the films patterned with a periodic squared arrangement of cylinders (S1) and with the design (S2). In thermocrystals, heat conduction is manipulated such that a wide range of phonons with relatively low frequencies match the phononic band gap frequencies of the periodic structure.

Hollow Microlattices: Energy Absorption and Damping Performance

Tobias A. Schaedler[1], Lorenzo Valdevit[2], Andrew Keefe[1], William B. Carter[1], Alan, J. Jacobsen[1]

[1] HRL Laboratories, LLC, Malibu CA, email: taschaedler@hrl.com
[2]University of California, Irvine, CA

The HRL Microlattice Technology represents a materials platform that enables fabrication of periodic lattice materials and structures combining aspects of traditional lithography, rapid prototyping, and printing[1]. By depositing various thin films materials (Au, Cu, Ni, SiO_2, poly($C_8H_4F_4$)) onto the polymer lattice templates and subsequently removing the polymer, hollow microlattices with densities from 0.5 kg/m^3 to 500 kg/m^3 are achieved[2]. The cellular architecture can be controlled precisely, enabling the design of new materials with unprecedented bulk properties (Figure 1).

At low relative densities, recovery from compressive strains of 50% and higher is observed, independent of lattice material and predictable by an analytical model[3]. At higher densities the crushing performance can be tailored by modifying the cellular architecture to achieve energy absorption properties of interest for protection applications[4].

Metallic or ceramic microlattices with reversible deformation behaviour display a novel energy absorption mechanism based on elastic buckling of hollow tubes, which is fundamentally different from conventional damping mechanisms. Utilizing this mechanism Ni-7%P microlattices have demonstrated a loss coefficient tan δ = 0.2, 10x higher than conventional nickel foams and on the order of viscoelastic polymers. The buckling based damping mechanism results in amplitude dependent damping as measured by dynamic mechanical analysis (Figure 2).

The reversible deformation behaviour is limited by the aspect ratio of the hollow tubes and microlattices with a wall thickness (t) to diameter (D) ratio larger than

$$\left(\frac{t}{D}\right)_{cr} = \frac{\sigma_{Y,S}}{E_S} \frac{0.25}{\theta - \sin^{-1}[(1-\epsilon_{max})\sin\theta]} \quad (1)$$

deform like conventional cellular materials. The crushing performance of hollow nickel microlattices with a larger aspect ratio is shown in Figure 3. The energy absorption behaviour can be tailored to a specific protection scenario and the transmitted stress can be adjusted to the injury threshold to enable maximum energy absorption while mitigating injuries.

In conclusion, hollow microlattice materials show promise for acoustic, vibration and shock damping.

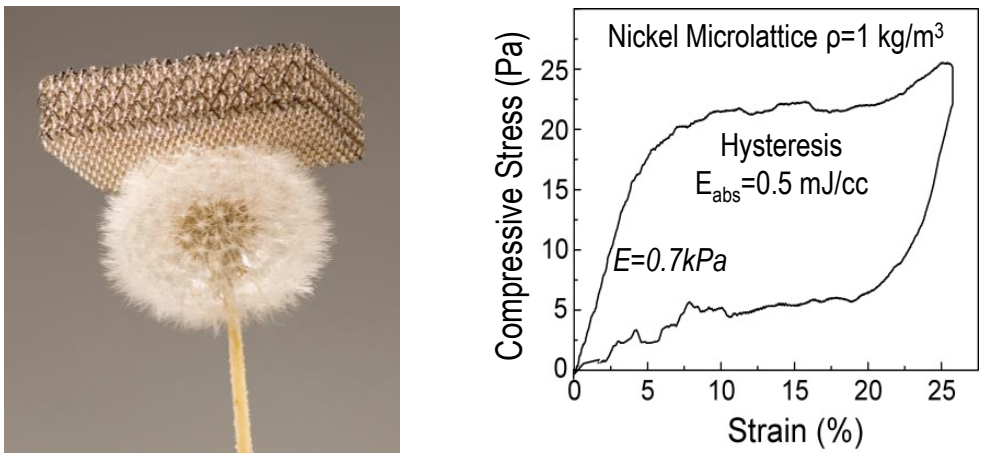

Fig. 1: Ultralight Hollow Nickel Microlattice and stress-strain curve measured in compression

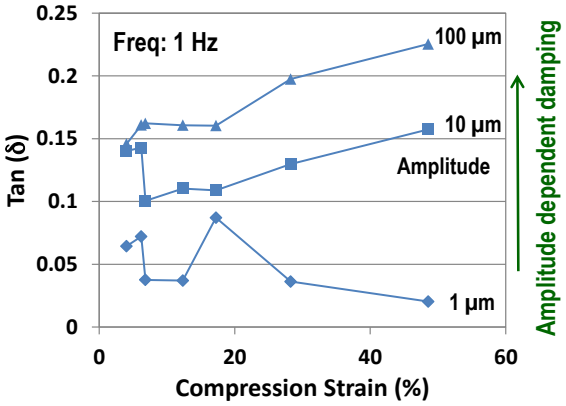

Fig. 2: Dynamic mechanical analysis (DMA) measurements of an ultralight hollow nickel microlattice at different levels of pre-compression showing amplitude dependent damping.

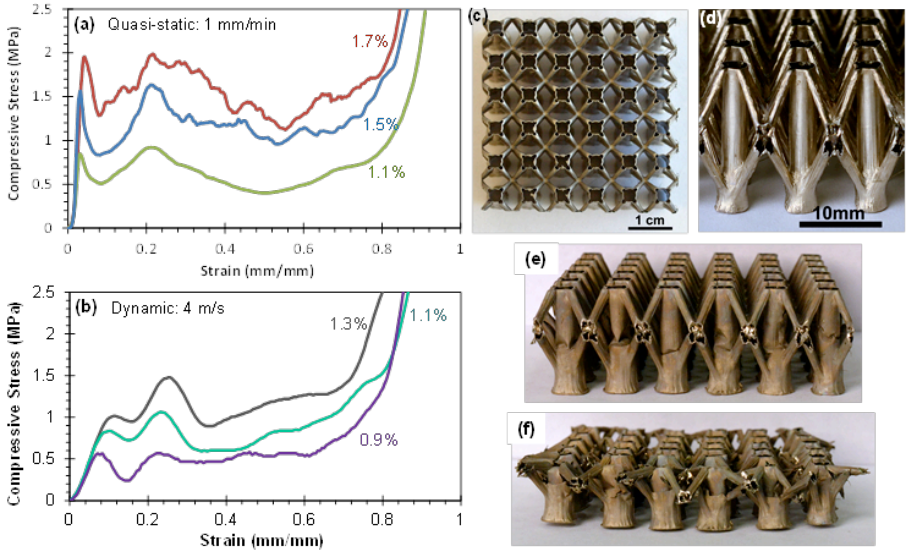

Fig. 3: (a) Quasi-static and (b) dynamic compression response of hollow nickel microlattices with vertical posts and relative densities of 0.9 – 1.7%. (c) Top and (d) side view before deformation; (e) ~10% and (f) 50% compressed microlattice.

References:

[1] A.J. Jacobsen, W.B. Carter, S. Nutt, *Advanced Materials* ***19***, 3892 (2007)

[2] K.J. Maloney, C.S. Roper, A.J. Jacobsen, W.B. Carter, L. Valdevit, T.A. Schaedler, *APL Materials* **1**, 022106 (2013)

[3] T. A. Schaedler, A. J. Jacobsen, A. Torrents, A. E. Sorensen, J. Lian, J. R. Greer, L. Valdevit, W. B. Carter. *Science* **334**, 962 - 965, (2011)

[4] T.A. Schaedler, C.J. Ro, A.E. Sorensen, Z. Eckel, S.S. Yang, W.B. Carter, A.J. Jacobsen. *Adv. Eng. Materials* DOI: 10.1002/adem.201300206 (2014)

Optimal design of stiff and lossy multiphase cellular materials

Alireza Asadpoure, Lorenzo Valdevit[1]

[1] *Department of Mechanical and Aerospace Engineering, University of California Irvine, Irvine, CA, USA*
valdevit@uci.edu

Abstract: In this presentation, we study the optimal design of stiff/lossy cellular materials for vibration damping. A visco-elastic material with complex elastic moduli is utilized to model the dissipative phase. The Bloch-Floquet theorems can then be applied to obtain damping capacity of the periodic multiphase domain, which allows investigation of the effect of wave directionality, architecture and intrinsic material on the effective damping. A classic metric for vibration damping of plates is optimized.

Introduction

Recent advances in manufacturing allow fabrication of single and complex multi-phase cellular materials with unprecedented topologies. Optimal design of these topologies could potentially result in unprecedented performance in a number of metrics. The powerful technique of topology optimization (whereby the optimal arrangement of a number of phases – including voids – within a design domain is sought to maximize a prescribed performance metric subject to prescribed constraints) is an ideal tool for the optimal design of periodic architected materials. Although stiffness optimization of two-phase lightweight structures and materials has been extensively investigated, the application of topology optimization to more complex objective functions in multi-phase material systems is still in its infancy. One of the subjects attracting interests lately is the optimal design of materials for vibration damping. For this application, ideal combinations of high stiffness, low density and high loss coefficient are desirable. As these combined attributes are not available in a single monolithic material, an interesting solution is the design of a multi-phase cellular material combining a stiff phase (a metal or a ceramic), a dissipative phase (an elastomer) and void space. The effective stiffness of the cellular material is easily calculated with homogenization theory; the Bloch-Floquet approach can then be utilized to analyze the dispersion characteristics and then estimate the damping capacity of the periodic architecture for waves traveling through the medium along any direction[1]. Based on this methodology, we present a topology optimization problem for the maximization of a classical figure of merit for stiff, light and lossy plates.

Governing equations

In an elastic medium, dynamical equilibrium takes the following form:

$$\nabla \boldsymbol{C}(\boldsymbol{x}) \nabla_{sym}\big(\boldsymbol{u}(\boldsymbol{x},t)\big) = \rho(\boldsymbol{x})\ddot{\boldsymbol{u}}(\boldsymbol{x},t) \tag{1}$$

where $\rho(\boldsymbol{x})$ is the material mass density at point $\boldsymbol{x}$, $\boldsymbol{u}(\boldsymbol{x},t)$ is displacement vector at point $\boldsymbol{x}$ and time t, $\boldsymbol{C}(\boldsymbol{x})$ is the stiffness tensor at point $\boldsymbol{x}$, $\ddot{\mathbf{u}}$ is the second derivative of displacement with respect to time, and ∇ and ∇_{sym} denote the gradient and symmetric gradient operators, respectively. For a periodic medium under harmonic oscillation, the Bloch[2] and Floquet[3] theorems provide a solution to (1) of the form:

$$\boldsymbol{u}(\boldsymbol{x},t) = \tilde{\boldsymbol{u}}(\boldsymbol{x}) e^{i(\boldsymbol{k}^T\boldsymbol{x}+\omega t)} \tag{2}$$

where ω is the frequency of the harmonic oscillation, $\boldsymbol{k}$ is the wavenumber, $\tilde{\boldsymbol{u}}(\boldsymbol{x})$ is an Ω_R periodic function, with Ω_R the unit cell of the material. Substituting (2) into (1) leads to solving an eigenvalue problem. A full description of the wave propagation characteristics of the material requires obtaining the dispersion curves within the first Brillouin zone. For a square unit cell of dimension a, the first Brillouin zone is $\left[-\pi/a \quad \pi/a\right]^d$, in d-dimensional $\boldsymbol{k}$-space. One can numerically solve the resulting

eigenvalue problem employing the Finite Element Method on the discretized unit cell, which leads to the following eigen-problem for k[1]

$$(\boldsymbol{K}_k(\omega) - k\boldsymbol{M}_k)\boldsymbol{d}_k = \boldsymbol{0} \tag{3}$$

where $\boldsymbol{K}_k$, $\boldsymbol{M}_k$, and $\boldsymbol{d}_k$ are equivalent stiffness matrix, mass matrix, and displacement vector, respectively, and $\boldsymbol{k} = k\boldsymbol{n}$, with $\boldsymbol{n}$ a unit vector with the desired direction within the first Brillouin zone.

In this problem, dissipative materials can be modelled by complex elastic moduli, whereby $\boldsymbol{C}(\boldsymbol{x})$ in eq. (1) becomes complex. In this situation, a wave vector k that is a solution to (3) is also complex, and its imaginary part represents a damped response, i.e. a spatially decaying wave. For such waves, the damping coefficient ($\tan\delta$) can be defined as:[1]

$$\tan\delta(\omega) = 2\|k"/k'\| \tag{4}$$

where k' and $k"$ are the real and imaginary parts of k. The advantage of using above formulation is that it can be easily applied to materials whose properties are frequency dependent. The accuracy of the model can be verified against analytical solutions for the simple topologies of Reuss and Voigt laminated composites under low frequency conditions. The well-known analytical solutions obtained with the correspondence principle[4] are shown as solid lines in Figure 1, with different points denoting different volume fractions of the metallic and viscoelastic phases. The open markers are obtained by solving E with homogenization theory; $\tan\delta$ is extracted with Eq. (4), using the wave vector solutions for longitudinal polarized waves at low frequency. In all simulations, Young's moduli of 20.0 GPa and $3.0 + i$ GPa ($\tan\delta = 0.33$) are used for the stiff and the lossy materials, respectively.

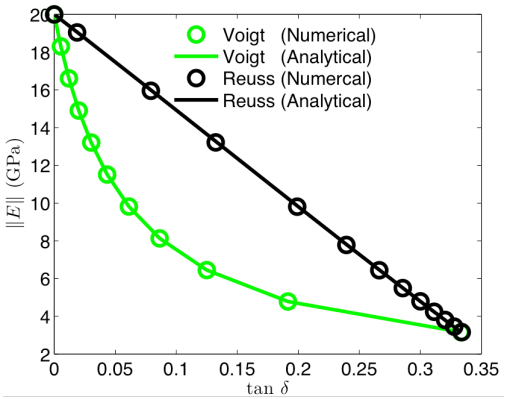

Figure 1 – E/$\tan\delta$ relationship for Voigt and Reuss laminated composites, for different volume fractions of the phases. Solid curves represent analytical visco-elasticity solutions[4], whereas open circles are numerical solutions obtained with (4) for longitudinally polarized waves at very low frequency.

Optimization problem

In the previous section, we presented a method to numerically compute wave damping for a multiphase periodic material using the Floquet-Bloch theorems. In order to optimize the material architecture, we need to choose meaningful metric for vibration damping. It can be shown[5] that in vibration of plates, the minimum eigenvalue of a plate is proportional to $E^{1/3}/\rho$. Hence, maximizing $E^{1/3}\tan(\delta)/\rho$ is desirable in most plate vibration applications. A formal optimization problem can then be stated as:

$$\max \frac{E^{\frac{1}{3}}(\tan\delta)_{min}}{\rho} \tag{5}$$

$$\tan\delta(\omega_i) = 2\|k_i"/k_i'\|, \quad i = 1, \dots, N_k \tag{6}$$

where N_k is the number of desired frequencies. Optimal solution to this problem will be presented for different relative densities of the hybrid cellular material and different wave directions.

References

[1] E Andreassen, J Jensen, *Journal of Vibration and Acoustics*, ***135***(4), 041015, (2013).
[2] F Bloch, *Zeitschrift für Physik*, **52**, 550–600, (1928).
[3] G Floquet, *Annales de l'Ecole Normale Supérieure*, **12**, 47–88, (1883).
[4] C Chen, R Lakes, *Journal of Materials Science*, **28**(16), 4299-4304, (1993).
[5] L Gibson, M Ashby, *Cellular Solids: Structure and Properties*, **2nd Edition**, (1999).

HYBRID POLYMER-NANOMETAL LATTICES

Craig A Steeves[1] and Glenn D Hibbard[2]

[1] *University of Toronto Institute for Aerospace Studies*
[2] *University of Toronto Department of Materials Science and Engineering*
csteeves@utias.utoronto.ca; glenn.hibbard@utoronto.ca

Abstract: This paper discusses both a novel fabrication technique for manufacturing lattices at the mm to cm scale, as well as some of the mechanical and dynamic properties of such lattices. The manufacturing route involves a combination of 3-D printing polymer preforms and electrodeposition of nanocrystalline metal. This process decouples the generation of complex geometries from the use of high-performance materials. Additionally, other physical properties of the lattice can be tailored, enabling other functional characteristics.

Lattice structures have many desirable characteristics, from novel dynamic performance to tailorable thermal expansion. However, the fabrication of lattices at a practical scale is often problematic because the geometric complexity excludes the use of many high performance materials: it is difficult to machine, form or forge high-strength materials. Three-dimensional printing offers a partial solution: it is straightforward to generate complex lattice geometries through this process. However, 3-D printing usually uses polymer, which is not an appropriate material for a structural application. This can be surmounted through the use of electrodeposited nanocrystalline metal to create a hybrid lattice structure. This paper will discuss, briefly, the fabrication process and some of the dynamic properties that can be tailored into such lattices.

The hybrid polymer-nanometal lattices that we have explored are configured as sandwich-like truss-core beams (see Figure 1).[1] These are fabricated by printing a polymer preform in the desired configuration. For the 3-D printing system we use, features down to approximately 100 microns can be printed accurately. In order to enable electrodeopsition of a metallic coating, the surface of the polymer preform must be metalised. This can be achieved through electroless deposition of a thin layer of metal (although this tends to produce relatively poor bonding) or through the application of a polymer-metal hybrid interlayer. Once the surface is appropriately prepared, nanocrystalline metal is electrodeposited through a pulse deposition process. The advantage of nanocrystalline metals arises because of the Hall-Petch effect: by reducing the grain size of the metal from the micron scale for a conventional metal to the nm size, the yield strength of the metal can increase by six of more times. For example, a conventional nickel typically has a yield strength of approximately 200 MPa; its nanocrystalline counterpart my have a yield strength of 1200 MPa or more.

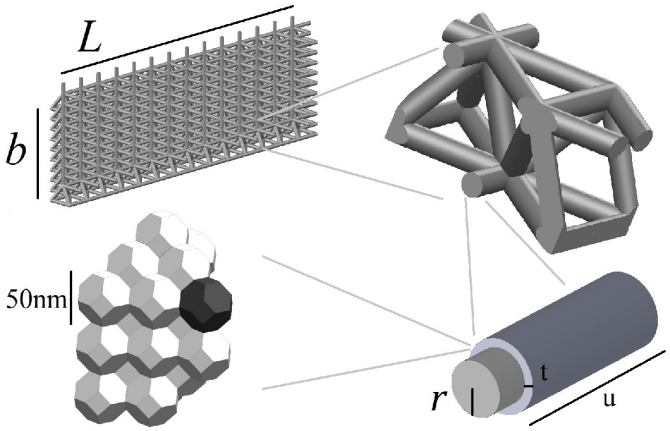

Figure 1: The hybrid polymer-nanometal lattices are tailorable at four length scales: the overall structural scale; the topology of the unit cell; the relative proportion of polymer and nanometal; and the atomic scale where the elemental composition and the grain size distribution can be selected.

This process enables the fabrication of structures that are very highly tailored to a particular application. First, it is possible to create structures that are very light, stiff and strong. More significantly, the geometric complexity of the lattice structure allows the design of additional functional properties.[2] Two examples that we are studying are tailored wave propagation and morphing. Floquet-Bloch analysis[3,4] of three-dimensional lattice structures, generating dispersion curves such as the one shown in Figure 2, shows that it is possible to design lattice geometries that have stop bands (or band gaps) in

their frequency response. This allows them to be used as wave propagation filters or vibration filters. However, the dispersion curve is a strong function of both geometry and material properties, specifically density and Young's modulus. Changing the ratio of density to modulus scales the dispersion curve. For typical structural materials, the ratio of density to Young's modulus lies in a fairly narrow band and hence the available scaling is limited. By contrast, the bending stiffness and effective density of the hybrid polymer – nanometal systems are different functions of the ratio of the strut radius to coating thickness, it is possible to design a broad range of effective modulus to density.

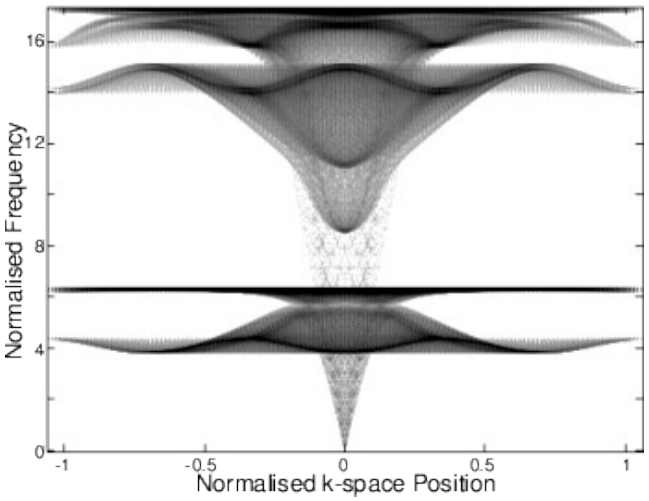

Figure 2: Sample Dispersion curve for a tetrahedral lattice with strut length to radius ratio of 50. This is a four-dimensional plot collapsed into two dimensions. By changing the effective stiffness and density, the dispersion curve can be stretched or compressed.

A second functional attribute that can be designed into hybrid lattices is temperature-driven morphing capability. The local thermal expansion of the hybrid lattice is determined by the ratio of metal to polymer material, and their individual expansion coefficients and moduli. By tailoring the size of the polymer preform and the thickness of the nanometal coating, we generate structures that deform in a controlled manner during thermal excursions. A photograph of a proof-of-concept structure is shown in Figure 3, before deformation and after deformation under an 80 C temperature change.

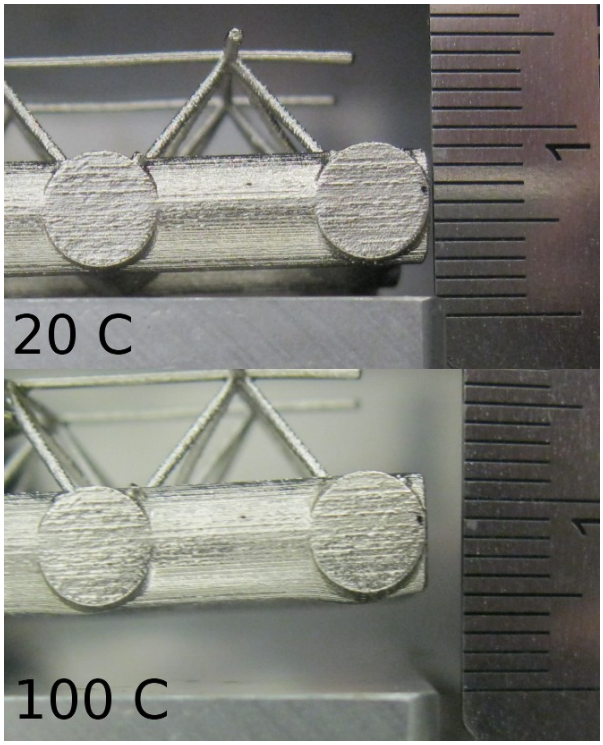

Figure 3: Proof-of-concept of thermally-driven morphing of a hybrid polymer-nanometal structure.

References

[1]L M Gordon, B A Bouwhuis, M Suralvo, J L McCrea, G Palumbo, and G D Hibbard. Micro-truss nanocrystalline Ni hybrids. *Acta Materialia*, **57**:932–939 (2009).

[2]A T Lausic, C A Steeves and G D Hibbard. Effect of grain size on the optimal architecture of electrodeposited metal/polymer microtrusses. To appear in *Journal of Sandwich Structures and Materials (*2014).

[3]A S Phani, J Woodhouse, and N A Fleck. Wave propagation in two-dimensional periodic lattices. *Journal of the Accoustical Society of America*, **119**(4):1995–2005 (2006).

[4]M Arya and C A Steeves. Bandgaps in octet truss lattices. In Proceedings of the 23rd Canadian Congress on Applied Mechanic s, Vancouver, Canada, 6-9 June 2011.

MULTIOBJECTIVE OPTIMIZATION OF A GRADED LATTICE FOR HIP REPLACEMENT: INTEGRATION OF MANUFACTURING AND BONE INGROWTH REQUIREMENTS

Damiano Pasini

McGill University, Mechanical Engineering, 817 Sherbrooke Street West, Montreal, H3A 0C3, Canada
damiano.pasini@mcgill.ca

Abstract: The multiobjective optimization of a Ti-6Al-4V lattice has been recently addressed for the development of a mechanically biocompatible implant for hip replacement. The material has a graded cellular microarchitecture tailored to simultaneously minimize bone resorption and implant micromotion, two conflicting objective functions. In this work, the optimization framework is extended to account for manufacturing constraints as well as bone ingrowth requirements that a femoral implant needs to satisfy.

Cementless or porous-coated implants are currently the gold standard in North America for total hip arthroplasty. These implants can wear and loosen over time, after which revision surgery is required. Revision surgery is a more complex procedure with increased technical difficulty, complications, mortality and a grown cost to the health care sector. The main causes for implant failure leading to revision surgery include the loss of bone stock from the loosening process and stress shielding [1,2]. One of the main culprits of stress shielding lies in the design of current hip implants in the market. Presently, all of them result in loss of femoral bone.

We have recently introduced an implant that can avoid bone resorption. Its hallmark lies in the material, a functionally graded open-cell lattice. The mechanical properties of the implant are in seamless harmonization to those of the bone tissue, thereby providing mechanical biocompatibility. In particular, the strain energy density at each site of the implant interface matches that of the trabecular and cortical bone that hosts it. Previous studies have demonstrated that tailoring the lattice microarchitecture can reduce bone resorption by 70% and interface shear stress by 53% compared to an implant with fully dense material [3-5]. Proof-of-concepts of femoral stems have been preliminary fabricated to prove the manufacturability of a graded microlattice and its potential to reduce bone resorption [4-5]. The implant design of these first investigations had a planar bulky shape with square lattice cells.

In this work, we extend the study to a 3d implant with a minimally invasive shape. Electron Beam Melting is used to build femoral stems made of a tetrahedron lattice. The solid material is Ti-6Al-4V, a biocompatible material commonly used in orthopedics, with properties: yield strength of 900 MPa, fatigue strength (at 107 cycles) of 600 MPa, Young's modulus of 120 GPa, and Poisson's ratio of 0.3.

The methodology encompasses aspects of multiscale mechanics, multiobjective optimization, and geometric mapping, all integrated into an optimization framework with embedded requirements of bone tissue formation and additive manufacturing. Starting with CT-scan data of a male patient femur (left of Figure 1), we reconstruct an accurate 3D model of the femur geometry with a realistic distribution of bone properties. For the lattice mechanics, we obtain the effective elastic and fatigue properties of the tetrahedron lattice via asymptotic homogenization with periodic boundary conditions applied to the unit cell. For the material optimization, we define sampling points within the implant domain (middle of Figure 1) and assign to each of them relative density as design variable. Bone resorption and implant micromotion are specified as objective functions that need to be concurrently minimized. The former is expressed by a functional appraising the relative difference in the local strain energy of bone between the preoperative and the postoperative situation, i.e. scenarios without and with implant in the femur. The latter is here defined as the probability of local interface failure, expressed by a global interface function index. This criterion is controlled by the interface stress at a given loading case, the vector of design variables, the interface area of the implant, and a local interface stress func-

tion defined with the multi-axial Hoffman failure criterion, which in turn assesses the local debonding that could occur along the bone-implant interface.

The design optimization is accomplished by implementing an in-house modified version of NSGAII, an evolutionary algorithm for multiobjective optimization. The result of this step is shown on the right of Figure 1. The relative density distribution refers to the anchor point of the Pareto front that represents an implant with minimum bone resorption.

The final step of the design procedure is the creation of the lattice microarchitecture. This is achieved via a set of in-house routines that map the relative density distribution into a graded lattice with density distribution reproducing the one shown in Figure 1 (right). The lattice consists of tetrahedron building blocks, mapped within a 3d minimally invasive implant. The lattice is tailored to ensure bone ingrowth requirements at the implant interface, with mean pore size below $400\mu m$ and porosity above 50%, as well as to respect manufacturing constraints that limit the minimum size of the lattice struts.

Preliminary results of in-vitro implantation of the femur into an artificial femur show the potential of exploiting architecture and properties of a graded lattice to develop a hip replacement implant that minimizes bone resorption.

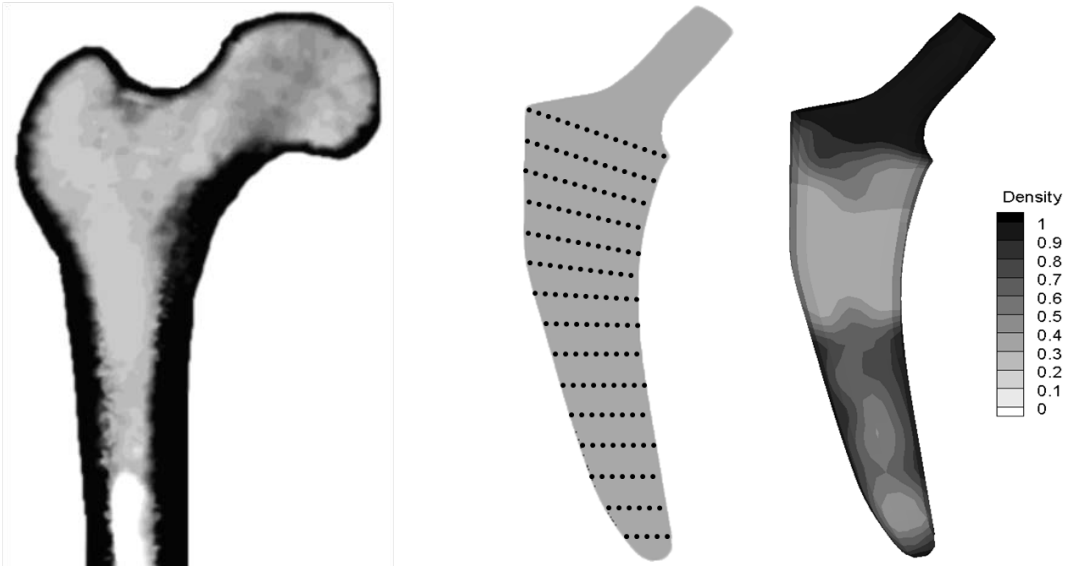

Figure 1. Left. CT scan data (relative density) of bone tissue femur of a 38 years old patient. Middle: Sample points defining the location of the design variables, i.e. the relative density, within the implant domain. Right: Optimum distribution of relative density for minimum bone resorption.

References

1. Glassman, A., J. Bobyn, and M. Tanzer, *New Femoral Designs Do They Influence Stress Shielding?* Clinical Orthopaedics and Related Research, 2006. **453**(12): p. 64-74.
2. Sundfeldt, M., et al., *Aseptic loosening, not only a question of wear: a review of different theories.* Acta Orthopaedica, 2006. **77**(2): p. 177-197.
3. Khanoki, S.A. and D. Pasini, *Multiscale Design and Multiobj ective Optimization of Orthopedic Hip Implants with Functionally Graded Cellular Material.* Journal of Biomechanical Engineering, 2012. **134**(3): p. 031004.
4. Khanoki, S.A. and D. Pasini, *Fatigue design of a mechanically biocompatible lattice for a proof-of-concept femoral stem.* Journal of the Mechanical Behavior of Biomedical Materials, 2013. **22**(0): p. 65-83.
5. Khanoki, S.A. and D. Pasini, *The Fatigue Design of a Bone Preserving Hip Implant with Functionally Graded Cellular Material.* ASME Journal of Medical Devices, 2013. **7**(2): p. 020908.

HARNESSING GEOMETRIC AND MATERIAL NON-LINEARITIES TO DESIGN TUNABLE PHONONIC CRYSTALS AND ACOUSTIC METAMATERIALS

Pai Wang, Filippo Casadei, Katia Bertoldi[1]

[1] *School of Engineering and Applied Sciences, Harvard University, Cambridge, Massachusetts 02138, USA, bertoldi@seas.harvard.edu*

Abstract: We investigate numerically and experimentally the effects of geometric and material nonlinearities introduced by deformation on the linear dynamic response of two-dimensional phononic crystals acoustic metamaterials. Our results not only show that deformation can be effectively used to tune the band gaps and the directionality of the propagating waves, but also reveal how geometric and material nonlinearities contribute to the tunable response of the systems. Our study provides a better understanding of the tunable response of phononic crystals and acoustic metamaterials and opens avenues for the design of systems with optimized properties and enhanced tunability.

Artificially structured composite materials that enable manipulation and control of elastic waves have received significant interest in recent years, not only because of their rich physics, but also for their broad range of applications, including wave guiding [1-7], cloaking [8] and noise-reduction [9-11]. An important characteristic of these heterogeneous systems is their ability to tailor the propagation of elastic waves through bandgaps - frequency ranges of strong wave attenuation. While in phononic crystals bandgaps are generated through Bragg scattering [12], in acoustic metamaterials localized resonances within the medium are exploited to attenuate the propagation of waves [13]. Thus, acoustic metamaterials are capable of manipulating waves with wavelength much larger than the structural features of the system [13] and have been succesfully exploited for vibration control [14-15], imaging [16], design of hybrid elastic solid [17] and thermal management [18].

Most of the phononic and acoustic metamaterial configurations proposed to date are characterized by a passive response and operate at fixed frequency ranges, limiting the number of applications. In an effort to design tunable systems, it has been shown that Bragg-type bandgaps can be controlled changing the geometry of the incusions [19] and using active constitutive materials [20-23]. Moreover, for acoustic metamaterials it has been demonstrated that tuning of functionalities has been achieved by altering the resonant frequency via piezo-shuntting [24] and fluid-structure interactions [25]

Here, I will show that mechanical loading can also be used as a robust mechanism for in situ tunability of soft and highly deformable two-dimensional phononic crystals and acoustic metamaterials. In particular, our results indicate that instability-induced transformations of the original pattern strongly affect both the position and width of the band gaps, paving the road to the design of a new class of phononic switches.

References

[1] A. Khelif, A. Choujaa, S. Benchabane, B. Djafari-Rouhani, and V. Laude, Appl. Phys. Lett. 84, 4400 (2004).
[2] M. Kafesaki, M. M. Sigalas, and N. Garcia, Phys. Rev. Lett. 85, 4044 (2000)
[3] A. Khelif, B. Djafari-Rouhani, J. O. Vasseur, P. A. Deymier, P. Lambin, and L. Dobrzynski, Phys. Rev. B 65, 174308 (2002)
[4] J.-H. Sun and T.-T. Wu, Phys. Rev. B 71, 174303 (2005)
[5] J.-H. Sun and T.-T.Wu, IEEE Ultrasonics Symposium 1, 673 (2006).
[6] J.-H. Sun and T.-T. Wu, Phys. Rev. B 76, 104304 (2007)
[7] J. O. Vasseur, A. Hennion, B. Rouhani, F. Duval, B. Dubus, and Y. Pennec, J. App. Phys. 101, 114904 (2007).
[8] S. Cummer and D. Schurig, New Journal of Physics 9, 45 (2007).
[9] D. Elser, U. L. Andersen, A. Korn, O. Glockl, S. Lorenz, C. Marquardt, and G. Leuchs, Phys. Rev.

Lett. 97, 133901 (2006).
[10] T. Elnady, A. Elsabbagh, W. Akl, O. Mohamady, V. M. Garcia-Chocano, D. Torrent, F. Cervera, and J. Snchez-Dehesa, Appl. Phys. Lett. 94, 134104 (2009),
[11] F. Casadei, L. Dozio, M. Ruzzene, and K. Cunefare, J. Sound. Vib. 329, 3632 (2010).
[12] C. Kittel, American Journal of Physics 35, 547 (1967).
[13] Z. Liu, X. Zhang, Y. Mao, Y. Zhu, Z. Yang, C. Chan, and P. Sheng, Science 289, 1734 (2000).
[14] F. Casadei, M. Ruzzene, L. Dozio, and K. Cunefare, Smart materials and structures 19, 015002 (2009).
[15] F. Casadei, B. Beck, K. A. Cunefare, and M. Ruzzene, Int. J. Solids Struc. 23, 1169 (2012).
[16] D. Bigoni, S. Guenneau, A. B. Movchan, and M. Brun, Phys. Rev. B 87, 174303 (2013),
[17] Y. Lai, Y. Wu, P. Sheng, and Z. Zhang, Nat. Mater. 10, 620 (2011).
[18] B. L. Davis and M. I. Hussein, Phys. Rev. Lett. 112, 055505 (2014)
[19] C. Coffaux and J. Vigneron, Physical Review B 64, 075118 (2001).
[20] J.-Y. Yeh, Physica B 400, 137 (2007).
[21] S. L. S. C. H. C. K.L. Jim, C.W. Leung, Applied Physics Letters 94, 193501 (2009).
[22] Y. L. Z. Hou, F. Wu, Solid State Commun. 130, 745 (2004).
[23] J. Robillard, O. B. Matar, J. Vasseur, M. S. P.A. Deymier, A. Hladky-Hennion, Y. Pennec, and B. Djafari-Rouhani, Appl. Phys. Lett. 95, 124104 (2009).
[24] A. Spadoni, M. Ruzzene, K. Cunefare, Journal of Intelligent Material Systems and Structures 20, 979 (2009)
[25]F. Casadei, K. Bertoldi, Journal of Applied Physics 115, 034907 (2014)

Active Acoustic and Structural Metamaterials

Amr M. Baz

[1] *University of Maryland, College Park, MD 20742*
email address: baz@umd.edu

Abstract: Active acoustic and structural metamaterials (*AASM*) are considered to synthesize extra-ordinary properties that do not exist in natural materials. Such metamaterials will be capable of morphing from one functional configuration to another based on mission requirements. This will enable the realization of acoustic cloaks, beam shifters, perfect absorbers, and/or perfect reflectors by simply programming a metamaterial platform to acquire the necessary properties without the need for changing the physical hardware of the platform itself.

Motivation

Extensive efforts are being exerted to develop a wide variety of acoustic and structural metamaterials that can effectively control the energy flow through various fluid media and/or structural materials. Most of these efforts are focused on passive metamaterials that have fixed material properties. This limits considerably the potential of this class of materials to perform effectively over a wide range of operating conditions. On the contrary, active metamaterials can provide viable means for functioning over wide frequency bands, adapting to varying external environment, and more importantly morphing from one functional configuration to another based on the mission requirements of the metamaterial. With such capabilities, it is envisioned that *AASM* can provide extra-ordinary properties that do not exist in natural materials as shown in Fig. 1. It is clear that natural materials cannot meet the demanding requirements of critical applications such as perfect absorbers, perfect reflectors, beam shifters, or acoustics cloaks. To achieve such extra-ordinary characteristics, the *AASM* can be programmed to map the desired functionally graded properties into its micro-structure simply by moving, as appropriately needed, around the corners and perimeter of the density-bulk modulus plan.

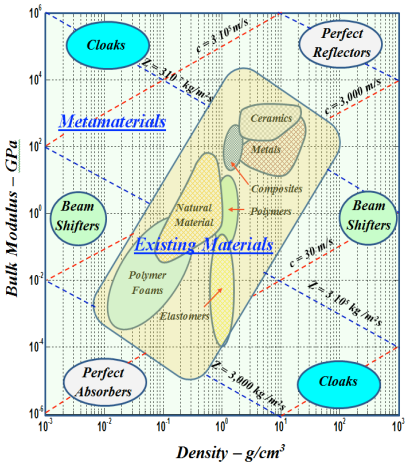

Fig. 1 - Regions of operation of existing materials, metamaterials, and potential applications in air (*c*= sound speed, *Z*=impedance)

Piezoelectric-Based *AASM*

This class of metamaterials is aimed at high frequency applications such as cloaking with an effective frequency band between 100-5000Hz. Such high capabilities are realized by configuring this class of *AASM* as 3D arrays of fluid cavities, separated by and provided with piezoelectric boundaries (Fig. 2). These boundaries control the stiffness of the individual cavity and in turn control its dynamical density and bulk modulus. All the cavities and boundaries look mechanically the same to facilitate manufacturing. However, with appropriate control, the individual piezo-boundaries can be programmed to achieve any desirable spectral and spatial distributions of the acoustical properties over the *AASM* volume. Such distributions would cover the range of acoustic properties between the two extreme ranges, as defined by the 3D transformation acoustics relationships near to and far from the object to be rendered acoustically invisible. Note that this object will be surrounded by the multi-layer donut-shaped *AASM* shown in Fig. 2. The basic building block (Fig. 2c) of the 3D *AASM* is a unit cell that consists of a main acoustic cavity to control the density and side Helmholtz cavities to control the bulk in the radial, tangential, and axial directions independently and simultaneously.

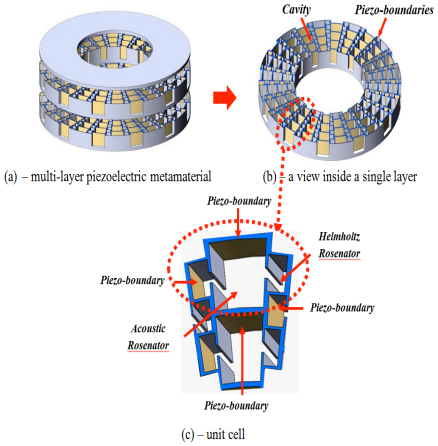

Fig. 2 - Three-dimensional piezoelectric-based metamaterial cloak

For the 1D *AASM* configuration shown in Fig. 3, the ability of the *AASM* to generate programmable distributions of dynamic densities that are orders of magnitude above and below ambient density is demonstrated. Such distributions are unachievable by natural materials or by passive metamaterial composites. Figure 22 displays the performance of a 1D *AASM* cell both in the time and frequency domains: densities of 0.33–22 times the ambient density are achieved and maintained over the frequency band 200-2,000Hz. This performance is limited by the dimensions of the *AASM* prototype, configured as a cylindrical cavity of 1" diameter and 1.5" length. In this project, wider ranges of acoustical properties will be achieved over wider frequency bands by manufacturing the 2D and 3D configurations of the *AASM* platform from smaller cavities using MEMS technology

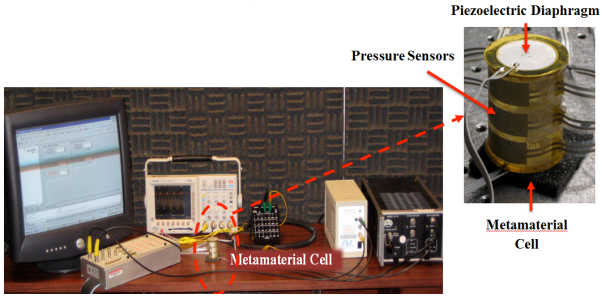

Fig. 3 - Experimental characterization of a prototype of the developed *AASM* cell

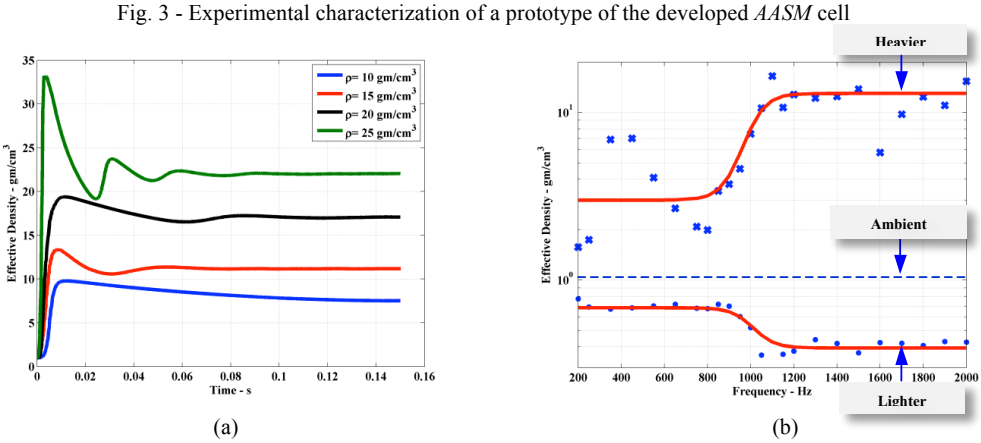

(a) (b)

Fig. 4. Experimental Time (a) and frequency (b) response of the developed 1D *AASM* cell

Closing Remarks

Active acoustic and structural metamaterials (*AASM*) with programmable properties present an attractive means for operating over wide frequency bands, adapting to varying external environment, and more importantly morphing from one functional configuration to another based on the mission requirements of the metamaterial. Prototypes of the active metamaterials have been demonstrated to have tunable density and/or bulk modulus with increasing or decreasing distributions over the material volume.

References

[1] A. Baz, "The structure of an active acoustic metamaterial with tunable effective density", *New Journal of Physics*, **11**, 123010 (2009).
[2] A. Baz, "An active acoustic metamaterial with tunable effective density", *ASME Journal of Vibration & Acoustics*, **132** (4), 041011 (2010)
[3] W. Akl and A Baz, "Stability analysis of active acoustic metamaterial with programmable bulk modulus", *Journal of Smart Materials and Structures*, **20** (12), 125010 (2011).
[4] W. Akl and A. Baz, "Analysis and experimental demonstration of an active acoustic metamaterial cell", *J. Appl. Phys*. **111** (4), 044505 (2012).
[5] W. Akl and A. Baz**,** "A technique for physical realization of anisotropic density matrices with application to acoustic beam shifters", *J. Appl. Phys*. **111** (2), 024907 (2012).
[6] W. Akl and A. Baz, "Multicell active acoustic metamaterial with programmable effective densities", *ASME Journal of Dynamic Systems, Measurement, and Control*, **134** (6) 061001-(1-11) (2012).
[7] W. Akl, A. Elsabbagh, and A. Baz, Acoustic metamaterials with circular sector cavities and programmable densities", *Journal of the Acoustical Society of America*, **132** (4), 2857-2865 (2012).

COUPLED VIBROACOUSTIC MODELING OF MEMBRANE-TYPE METAMATERIALS

Yangyang Chen, Guoliang Huang[1]

[1] *Department of Systems Engineering, University of Arkansas at Little Rock, Little Rock, Arkansas 72204, USA*
glhuang@ualr.edu

Abstract: Membrane-type Acoustic Metamaterials (MAMs) have demonstrated unusual capacity in controlling low-frequency sound transmission/reflection. In this paper, an analytical vibroacoustic membrane model is developed to study sound transmission behavior of the MAM under a normal incidence, by adopting point matching method. The accuracy and capability of the theoretical model is verified through the comparison with the finite element method. In particular, microstructure effects are quantitatively investigated. The developed model can be served as an efficient tool for design of such membrane-type metamaterials.

The prototype proposed by Yang et al.[1] now is recast into more general concept of MAMs, which have been suggested to possess excellent acoustic properties for low-frequencies sound insulation. Consider now a unit cell of a MAM, as shown in Fig. 1(a), where the deformable membrane is attached by an eccentrically circular mass in finite dimension. In the figure, the membrane is subject to initial uniform tension T per unit length. In the study, we focus on the sound transmission and reflection of the stretched MAM in a tube subject to a plane normal sound wave, as shown in Fig. 1(b). Perfectly absorbing boundary conditions are assumed in both ends of the tube so that there will be no multiple reflected waves to the MAM.

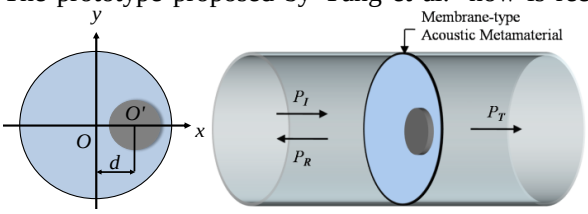

Figure 1: (a) MAM attached with an eccentric mass. (b) MAM subjected to a normal acoustic loading in a tube.

To properly capture effects of the finite mass on the small deformation of the membrane, the point matching scheme is applied by using distributed point forces along the interfacial boundary between the mass and the membrane. For the attached mass in finite dimension, the general rigid motion can be completely described by the translation and rotation. Based on the displacement continuity between the mass and the membrane on every collocation point, we can finally derive an eigensystem, from which natural frequencies and mode shape functions of the membrane can be obtained. Computed mode shapes of an MAM with a central mass and an eccentric mass are shown in Fig. 2 (a) and (b) for first three symmetric modes. Pressure field in the tube can be decomposed as plane waves and higher order waves. The out-of-plane displacement field can also be decomposed as the averaged displacement field and deviation displacement field. Based on out-of-plane velocity continuous condition between the air and the membrane, the piston-like (averaged displacement field) motion of the MAM is attributed to the 0th-order plane waves, and the deviation displacement field is attributed to the higher order scattered wave fields. The governing equation of coupled vibroacoustic modeling of the MAM can be finally obtained. To solve the integrodifferential equation, we use the modal superposition method such that the mode shape functions are selected as trail functions.

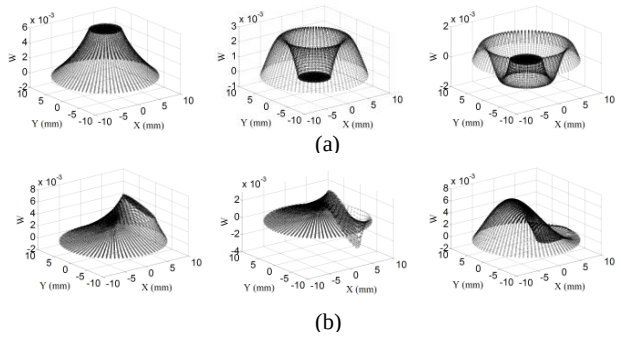

Figure 2: (a) Mode shapes of MAM with a central mass. (b) Mode shapes of MAM with an ecccentric mass.

To evaluate the developed model, acoustic property predictions of the MAM from the current model will be compared with those by using commercially available finite element (FE) code, COMSOL

Multiphysics. Figure 3 (a) illustrates the obtained intensity transmission coefficients of the MAM from the FE simulation and analytical results with a centric attached mass. It is observed that the acoustic behaviour of the MAM does not follow the prediction by the conventional mass density law, two transmission peaks are observed in the two lowest resonant frequencies and there is a dip frequency between them. The intensity transmission coefficient validations of the MAM with an eccentric mass are plotted in Fig. 3 (b). Theoretical results agree well with those from finite element simulations. A new transmission peak can be found from the figure, which is caused by the rotational motion of the mass. Two transmission valleys are formed between the first and the second transmission peaks and between the second and the third transmission peaks.

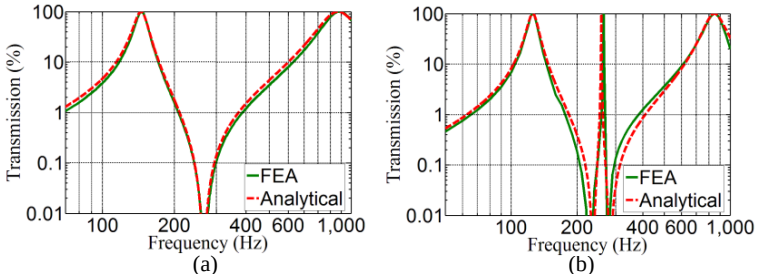

Figure 3: (a) Validation of transmissions of MAM with a central mass. (b) Validation of transmissions of MAM with an eccentric mass.

As we know, weight of the attached mass of the MAM is a key parameter of selecting the resonant frequencies for low-frequency acoustic transmission applications. Figure 4 shows effects of different weights of the central mass on the two peak frequencies and one dip frequency of the MAM. The mass geometry effects on the two peak frequencies and one dip frequency of the MAM are illustrated in Fig. 5. Figure 6 shows the membrane's pretension effect on the two peak frequencies and one dip frequency of the MAM. The membrane thickness effect on the two peak frequencies and one dip frequency of the MAM is studied in Fig. 7. Finally, Figure 8 shows the trend of the three peak frequencies with the change of the mass eccentricity. Different from existing models, the proposed model can provide highly precise analytical solutions of vibroacoustic problems of the MAM, in which the finite mass effects on the deformation of the membrane can be properly captured. The accuracy of the model is verified through the comparison with the FE method.

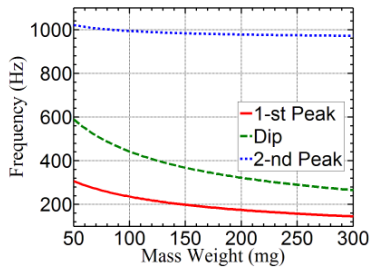

Figure 4: Effects of mass's weight to peak and dip frequencies of MAM with a central mass.

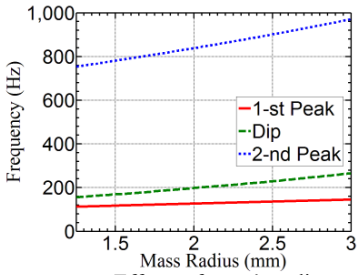

Figure 5: Effects of mass's radius to peak and dip frequencies of MAM with a central mass.

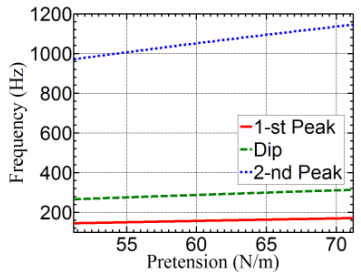

Figure 6: Effects of mass's pretension to peak and dip frequencies of MAM with a central mass.

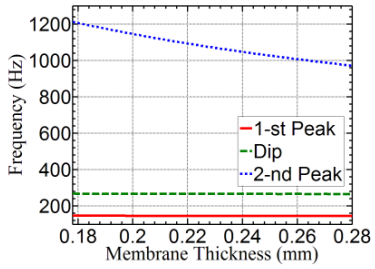

Figure 7: Effects of membrane's thickness to peak and dip frequencies of MAM with a central mass.

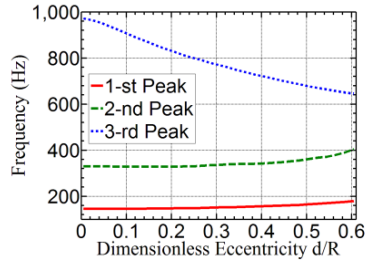

Figure 8: Effects of mass's eccentricity to peak frequencies of MAM with an eccentric mass.

References

[1] Z. Yang et.al, Phys. Rev. Lett. **101**, 204301 (2008).

NOTES

NOTES

NOTES

NOTES

NOTES

NOTES

NOTES